出國報告（出國類別：其他）

赴英參加第九屆應用能源國際研討會(ICAE2017)出國報告

服務機關：核能研究所
姓名職稱：李灝銘　副工程師
派赴國家：英國
出國期間：106 年 8 月 20 日~106 年 8 月 26 日
報告日期：106 年 9 月 11 日

摘　要

本所「智慧熱管餘熱回收節能關鍵技術開發」科技計畫係針對市場缺口開發耐腐蝕熱管熱交換器，本次出國即是將部分研發成果與國外專家學者交流、汲取國外經驗並了解國際現況，同時展現我國研究能量。本次參加的第九屆應用能源國際研討會(9th International Conference on Applied Energy, 以下簡稱為 ICAE2017)，乃 Elsevier 雜誌下之知名期刊 Applied Energy 主辦的年會，今年在英國卡地夫(Cardiff)舉行，本次會議共有來自全球 50 多個國家的專家學者與會，發表 650 篇以上的論文。

筆者本次發表兩篇論文，一篇為本所在工業節能領域上高效能熱管的研發成果 A mathematical model for estimation of the maximum heat transfer capacity of tubular heat pipes with water and mesh wicks，另一篇為本所在溫室效應氣體減量技術的研發成果 Perfluorocompounds emission control with thermal plasma torches，兩篇論文之全文收錄於本報告之附錄。另外榮幸受邀擔任「熱傳提升、熱交換器及熱管」主題的兩場會議主持人，筆者藉開場時簡介本所能源研發現況，增加我國能源研發國際能見度與知名度，同時跟與會者交流，成功建立一些新國際合作網絡。

英國 BEIS 首席科學顧問 Prof. Loughhead，於大會主題演講時介紹英國未來電力規劃，鼓勵與支持相關新技術的發展之外，不輕易放棄既有發電方法(如燃煤與核電)；新技術除創新之外，重視供應安全與經濟成本；研擬政策時將民眾接受度、工業因應策略、執行方法、環保目標等納入考量，相當客觀、理性與全面，值得參考。

美國普渡大學研究和合作夥伴執行副總裁 Prof. Garimella，於主題演講說明各種資通訊目前與未來的熱管理問題，介紹多種新式的熱管理技術，強調未來電子產品的熱管理要求日漸嚴苛，以往單一學門或領域的獨立研究已難以滿足產業的現實需求，未來必須跨學門與領域合作，以系統全面思維發現及解決問題。

在熱管研發部分，熱管研發雖然已有歷史，但仍有一些新型熱管持續被開發與研究。迴路式熱管是個有效的電子散熱元件，工作流體的填充率對迴路熱管的散熱性能影響至為關鍵，但如何優化仍須進一步研究。另一方面，熱管芯的幾何形狀會影響熱管的傳熱量，研發雖可透過數值模擬進行優化設計，然而實務上必須考量製作方法的可行性與製作成本經濟性。

有機朗肯循環(Organic Rankine Cycle, ORC)是目前餘熱回收發電中被期待的關鍵技術之一。本次研討會上共有 13 篇 ORC 相關之論文，被應用在許多領域或場合，例如交通的柴油引擎廢熱回收發電、太陽熱能利用、微渦輪機汽電共生、空氣儲能、LNG 氣化程序、地熱應用等，於本報告中有簡要介紹。

目　次

(頁碼)

一、目　的

我國工業餘熱每年估計有 3.9 百萬公秉油當量，佔全國工業能源總需求量的 9.2%，其中溫度低於 250^{o}C 的低階餘熱佔了 75% [1]。若上述低階餘熱可以完全回收，每年可以減少 800 萬噸 CO_2 排放。上述低階餘熱回收利用就理論而言不難，但應用溫度區間(T<250^{o}C)，正好遇到酸露點(T<~150^{o}C)腐蝕的現實問題，市場上出現技術缺口。本所「智慧熱管餘熱回收節能關鍵技術開發」科技計畫，正在開發適合上述情境應用的耐腐蝕熱管熱交換器。本次出國即是將部分研發成果與國外專家學者交流、汲取國外經驗並了解國際現況。本次參加的第九屆應用能源國際研討會(9th International Conference on Applied Energy 以下簡稱為 ICAE2017)，乃 Elsevier 雜誌下之知名期刊 Applied Energy 主辦的年會，今年在英國卡地夫(Cardiff)舉行，本次會議共有來自全球 50 多個國家的專家學者與會，發表 650 篇以上的論文。筆者從事前瞻工業節能技術開發，奉派參加此會議，發表研發成果展現我國研究能量，同時藉由參與 ICAE 系列研討會，窺探國際研發趨勢，作為我國工業節能技術發展方向之參考；強化國際研發人脈，嘗試建立合作管道，加速科技研發進程。

二、過　程

第九屆應用能源國際研討會(ICAE2017)，於 2017 年 8 月 21~24 日於英國卡地夫舉行。本次公差共計 7 日，行程如**表 1** 所示。20 日啟程經荷蘭阿姆斯特丹機場轉機，21 日抵達英國卡地夫(Cardiff)，同日至 ICAE2017 會場註冊並了解會場環境，22~24 日等三天參加會議，25 日回程，26 日返抵國門。

表 1：公差行程與主要活動說明

日期	地點	主要活動說明
8/20 (日)	桃園→荷蘭阿姆斯特丹機場	啟程及轉機
8/21 (一)	荷蘭阿姆斯特丹機場→英國卡地夫	抵達旅館報到 至會場註冊 熟悉會場環境 了解大會資訊與議程
8/22 (二)	英國卡地夫	參加研討會 聽邀請演講 海報發表論文一篇(附錄一) 主持會議一場
8/23 (三)	英國卡地夫	參加研討會 口頭發表論文一篇(附錄二) 參加大會晚宴
8/24 (四)	英國卡地夫	參加研討會 主持會議一場
8/25 (五)	英國卡地夫→荷蘭阿姆斯特丹機場	旅館退房、回程及轉機
8/26 (六)	荷蘭阿姆斯特丹機場→桃園	返抵國門

本次 ICAE2017 研討會計有全球 50 多個國家的專家學者與會，發表論文超過 650 篇，分成 108 場次口頭發表與 2 場海報發表，大會另外安排了 4 場專題演講與 6 個論壇，大會議程簡表如**表 2** 所示，細部議程由於頁數過多不在本報告中列出，有興趣讀者可以參考文獻[2]或至 ICAE2017 官網http://www.applied-energy.org/icae2017/查詢。我國共計 5 位專家學者與會，除筆者外，有 3 位大學教授，另一位來自金屬中心。

表 2：ICAE2017 研討會簡易議程[2]

Registration: Aug 21, 14:00-16:00; Aug 22-23, 8:00-17:00; Aug 24, 8:00-12:00

Editorial Board Meeting: Aug 21, 17:30-19:00, Caernarfon suite, Mercure Cardiff Holland House Hotel

Welcome reception: Aug 21, 19:00-21:30, Cardiff City Hall, Cathays Park, Cardiff, CF10 3ND

Time	Day 1: Aug 22										
09:00-09:10	Opening										
09:10-09:50	Keynote 1										
09:50-10:30	Keynote 2										
10:30-10:50	Tea/Coffee Break										
10:50-11:30	Keynote 3										
11:30-12:10	Keynote 4										
12:10-13:00	Lunch										
13:00-13:40	Poster Session I										
Afternoon	1-A3	1-B3	1-C3	1-D3	1-E3	1-F3	1-G3	1-H3	1-I3	1-J3	1-K3
13:40-15:20	RE	RE	IES	ES	MT&S	EMEC	EMEC	CECT	RE	CECT	PS
15:20-15:50	Tea/Coffee Break										
Afternoon	1-A4	1-B4	1-C4	1-D4	1-E4	1-F4	1-G4	1-H4	1-I4	1-J4	1-K4
15:50-17:30	RE	RE	IES	ES	MT&S	EMEC	EMEC	CECT	RE	CECT	PS
Time	Day 2: Aug 23										
Morning	2-A1	2-B1	2-C1	2-D1	2-E1	2-F1	2-G1	2-H1	2-I1	2-J1	2-K1
08:10-09:50	RE	RE	IES	ES	MT&S	EMEC	EMEC	CECT	MT&S	CECT	PS
09:50-10:20	Tea/Coffee Break										
Morning	2-A2	2-B2	2-C2	2-D2	2-E2	2-F2	2-G2	2-H2	2-I2	2-J2	2-K2
10:20-12:00	RE	RE	IES	ES	MT&S	EMEC	EMEC	CECT	MT&S	CECT	PS
12:00-13:00	Lunch										
13:00-13:40	Poster Session II										
Afternoon	2-A3	2-B3	2-C3	2-D3	2-E3	2-F3	2-G3	2-H3	2-I3	2-J3	2-K3
13:40-15:20	RE	RE	IES	ES	MT&S	EMEC	EMEC	CECT	EMEC	CECT	PS
15:20-15:50	Tea/Coffee Break										
Afternoon	2-A4	2-B4	2-C4	2-D4	2-E4	2-F4	2-G4	2-H4	2-I4	2-J4	2-K4
15:50-17:30	RE	RE	IES	ES	MT&S	EMEC	EMEC	CECT	RE	CECT	PS
19:00-22:00	Conference Banquet										
Time	Day 3: Aug 24										
Morning	3-A1	3-B1	3-C1	3-D1	3-E1	3-F1	3-G1	3-H1	3-I1	3-J1	3-K1
08:10-09:50	RE	RE	IES	ES	MT&S	EMEC	EMEC	CECT	RE	CECT	
09:50-10:20	Tea/Coffee Break										
Morning	3-A2	3-B2	3-C2	3-D2	3-E2	3-F2	3-G2	3-H2	3-I2	3-J2	3-K2
10:20-12:00	RE	RE	IES	ES	MT&S	EMEC	EMEC	CECT	RE	IES	
12:00-13:00	Lunch										
Afternoon	3-A3	3-B3	3-C3	3-D3	3-E3	3-F3	3-G3	3-H3	3-I3	3-J3	3-K3
13:00-14:40	RE	RE	IES	ES	MT&S	EMEC	EMEC	CECT	EMEC	CECT	
14:40-15:00	Tea/Coffee Break										
Afternoon	3-A4	3-B4	3-C4	3-D4	3-E4	3-F4	3-G4	3-H4	3-I4	3-J4	3-K4
15:00-17:00	RE	RE	IES	ES	MT&S	EMEC	EMEC	CECT	EMEC	EMEC	

MT&ES = Mitigation technology and energy storage; CECT=Clean energy conversion technology; EMEC=Energy management, policy and economics; ES=Energy sciences; IES=intelligent energy system; RE=Renewable energy; PS=Panel Session

ICAE2017 研討會主要議程可區分為 6 大類：

1. 減排技術和能源儲存(Mitigation technology and energy storage, MT&MS)、
2. 清潔能源轉換技術(Clean energy conversion technology, CECT)、
3. 能源管理/政策與經濟學(Energy management, policy and economics, EMEC)、
4. 能源科學(Energy sciences, ES)、
5. 智慧能源系統(Intelligent energy system, IES)、及
6. 可再生能源(Renewable energy, RE)。

同一時段有 10 場會議同時舉行，基於筆者節能技術與生質能的研究背景，本次會議以參加能源科學或可再生能源等兩類議程為主要選擇，即**表 2** 中代碼 ES 與 RE 者。

筆者本次發表兩篇論文，第一天下午海報發表本所在溫室效應氣體減量技術的研發成果，題目為以熱電漿火炬控制全氟化物排放(Perfluorocompounds emission control with thermal plasma torches)，內文說明全氟化物的溫室效應及減排之必要性，同時展示相關正面的實驗結果，最後闡述進一步節能的可行方向，論文全文詳見**附錄一**。

第二天早上口頭發表一篇在工業節能領域上高效能熱管的研發成果，題目為管狀網目結構水熱管最大熱傳量之數學模型(A mathematical model for estimation of the maximum heat transfer capacity of tubular heat pipes with water and mesh wicks)，熱管最大熱傳量理論的研究已有相當歷史，但本文彙整文獻後發現一些方程式有誤，經歸納與驗證後建議可信的方程式，並進行案例分析與討論，論文全文詳見**附錄二**。

另外，筆者(英文姓名 HowMing Lee)榮幸受大會邀請，擔任「熱傳提升、熱交換器及熱管」主題的兩場會議主持人，分別在第一天下午與第三天早上(如**表 3**)。筆者在每場會議開場前自我介紹，藉機簡述本所能源研發方向與現況，讓與會者初步了解本所與我國的能源技術發展現況。主持會議過程，與講者及與會者多有互動與交流，同時結識許多新的專家學者，有助增加我國能源研發國際能見度與知名度。

表 3：榮幸擔任兩場會議主持人

Day 1 Oral Presentations

Room: Kidwelly suite Session Name: Heat transfer enhancement, heat exchangers and heat pipe Session Chair: Rebei Bel Fdhila, HowMing Lee			
Time	**Paper ID**	**Author**	**Paper Title**
15:50-16:10	13	Wenlong Cheng, Yu-hang Peng	Experimental investigation on the effect of heat transfer enhancement of vacuum spray flash evaporation cooling using Al2O3–water nanofluid
16:10-16:30	31	Ya Ge, Zhichun Liu, Wei Liu, Feng Shan, Fang Yuan, Rui Long	Multi-objective arrangement optimization of a tube bundle in cross-flow using CFD and genetic algorithm
16:30-16:50	39	Yin Zhang, Mingshan Zhang, Zhiyuan Wei, Shurui Guo, Enshen Long	Outdoor air thermal plume simulation of layer-based VRF air conditioners in high-rise buildings
16:50-17:10	307	Agus Sasmito, Mahmoud AlZoubi, Ali Ghoreishi, Ferri Hassani	Intermittent freezing concept for energy saving in artificial ground freezing systems
17:10-17:30	446	Bernard, Ming Chian Yew, Ming Kun Yew, Yusof Farazila, Naqiuddin Haziq	Numerical analyses of the novel geometrically graded micro-channel heat sink

Day 3 Oral Presentations

Room: Kidwelly suite Session Name: Heat transfer enhancement, heat exchangers and heat pipe Session Chair: HowMing Lee, Dongmei Pan			
Time	**Paper ID**	**Author**	**Paper Title**
10:20-10:40	453	Yiji Lu, Yuqi Huang, Rui Huang, Xiaoli Yu, Tony Roskilly	Study on the thermal interaction and heat dissipation of cylindrical Lithium-Ion battery cells
10:40-11:00	603	Yiping Cao, Qi Xiao, Yuansheng Lin, Qiuwang Wang	Simulation of the printed circuit heat exchanger for S-CO2 by segmented methods
11:00-11:20	541	Isam Janajerh, Raed Hashaikeh, Farah Ahmed, Khadija Elqadi	Low energy membrane distillation: a numerical study on the role of conductive spacers
11:20-11:40	69	Mengjie Song, Ning Mao, Xuanjie Wang, Chaobin Dang, Wenke Zou	Review on frost layer thickness measurement and calculation
11:40-12:00	751	Pedro Dinis Gaspar, Pedro Dinho da Silva, Luís Pires, Diogo Carrilho, José Nunes	Quantification of the thermal resistance variation in evaporators surface due to ice formation

大會 8/22 日上午，以 4 場主題演講(keynote speech)揭開大會序曲，講者、職稱及演講題目列於**表 4**，講者來自英國、德國、美國、新加坡等世界各地，講題內容主要在展望現況與啟發未來，前兩場演講相當精彩，略述於後。

表 4：ICAE2017 大會邀請四場演講(keynote speech)之講者與其講題

場次	講者	職稱	講題	照片
1	Prof. John Loughhead	英國 BEIS 首席科學顧問	Future Trends in UK Energy –What Are Major Development Areas for Future UK System?	
2	Prof. Suresh V. Garimella	美國普渡大學 研究和合作夥伴 執行副總裁	Energy Use in Information and Communications Technologies: The Role of Thermal Management	
3	Prof. Siaw Kiang Chou	新加坡大學教授 新加坡工程師學會 前會長	East Asia Energy Policy: Research & Outlook	
4	Prof. Roland Span	德國Ruhr大學 機械工程學院院長 熱力學主席	Closed Carbon Cycle Economy	

第一場主題講題為 “Future Trends in UK Energy –What Are Major Development Areas for Future UK System?” 講者Prof. John Loughhead目前是英國Department for Business, Energy and Industrial Strategy (BEIS, 商業、能源和工業戰略部)的首席科學顧問。在此之前，他曾擔任能源與氣候變化部(Department of Energy and Climate Change, DECC)的首席科學顧問。他在英國和國際上擔任過許多重要角色，包括英國能源研究中心執行總監(UKERC, UK Energy Research Centre)和 Alstom 技術與智慧產權公司副總裁。職業生涯主要在電子和電力行業的工業研究和開發，包括先進的大功率工業燃氣輪機、新式能源轉換系統、航太飛行器的熱管理、發電/輸電設備/電子控制系統的電器及材料開發等。Prof. Loughhead 畢業於帝國理工學院機械工程，也是皇家工程學院、機械工程師學會、倫敦瑪麗皇后大學、及英國和澳大利亞國家工程學院等院士，是位極具學術聲望的專業工程師。英國對於未來電力的規劃，除了鼓勵與支持相關新技術的發展之外，不輕易放棄既有發電方法(如燃煤與核電)；另外同步重視供應安全與經濟成本兩方面(如**圖 1 左**)。將民眾接受度、工業因應策略、執行方法、污染物環保目標等納入能源政策制定中一環(如**圖 1 右**)，可發現十分客觀、理性與全面，無怪乎可制定出

具說服民眾的政策。

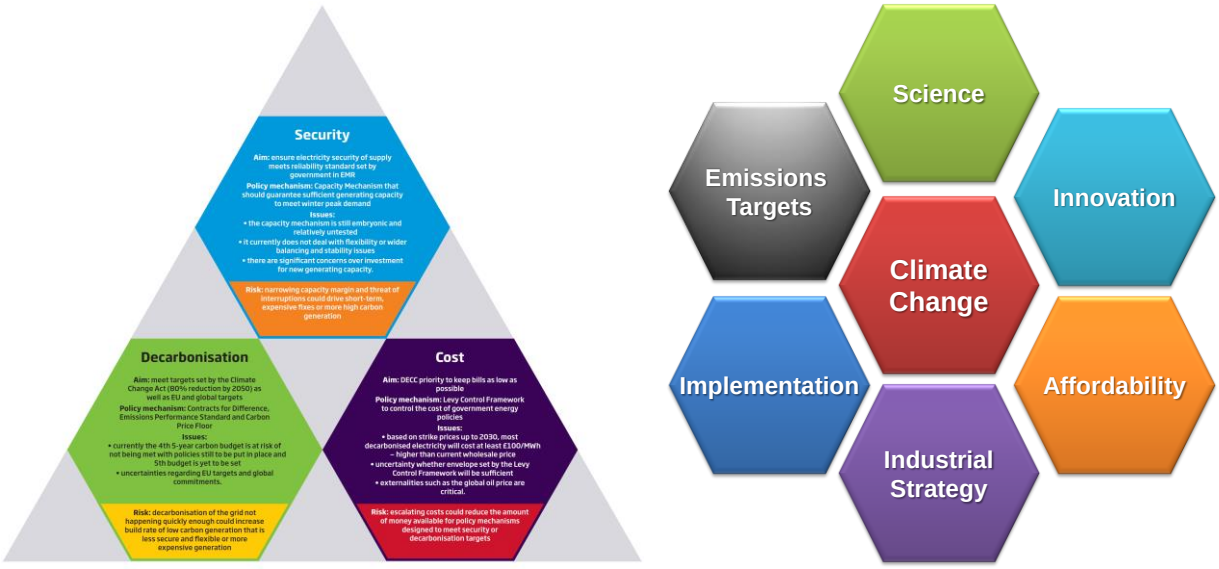

圖 1：英國電力系統與能源規劃策略—降低碳排、安全與成本等三者應全面考量

第二場主題講題為 “Energy Use in Information and Communications Technologies: The Role of Thermal Management”，講者 Prof. Suresh Garimella 是美國普渡大學研究和合作夥伴執行副總裁、Goodson 傑出機械工程教授，同時擔任國家科學基金會冷卻技術研究中心主任。他於 1985 年取得印度理工學院馬德拉斯學士學位，1986 年獲得俄亥俄州立大學碩士學位，1989 年榮獲加州大學柏克萊分校博士學位。他曾擔任美國國務院美洲能源與氣候夥伴關係高級研究員(ECPA)五年(2011-2016)，被歐巴馬總統提名推動相關清潔能源發展。Prof. Garimella 擔任多個知名期刊的編輯，榮獲美國科學促進會(AAAS, the American Association for the Advancement of Science)和美國機械工程師學會(ASME, the American Society of Mechanical Engineers)的會士(Fellow)。曾榮獲多項大獎，如 2014 ASME Charles Russ Richards 紀念獎、2011 NSF Alexander Schwarzkopf 技術創新獎、2010 ASME 熱傳紀念獎、2010 IIT Madras 傑出校友獎、ASME Allan Kraus 熱管理獎、及 2004 ASME Gustus L. Larson 紀念獎等。

由於電子設備和相關數位世代的迅速成長，數據中心(data center)佔全球電力需求的很大比例。儘管能源消費總量迅速增長，但大型數據中心和工作站的現有空調與冷卻技術，總體能源消耗卻是不合理地低效，估計約佔 40%以上。Prof. Garimella 簡報時提出一些數據，全球有超過 26 億網路使用者，資料中心的 CO_2 排放量佔全球排放量的 0.2%，總碳排放量約 80 百萬噸，且持續快速增加，估計 2020 年時，碳排放量會增加 4.25 倍，達到 340 百萬噸。國內

亦曾有報導[3]，全球所有的資料中心在 2011 年的耗電量占全世界用電量的 1.3%，2012 年上升到 1.5%。而國內彰化有 Google 資料中心一座；還有大大小小數量眾多的資料中心，因此資料中心的用電與節電必須重視。

面對未來電子產品的熱管理要求日漸嚴苛，以往單一學門或領域的獨立研究，已難以滿足產業的現實需求，Prof. Garimella 認為必須技術整合與跨領域合作，如電子、熱傳、材料、製作等通力合作，在 IC 設計階段時就必須開始合作，而非等到 IC 製作後才來解決散熱問題。

液體冷卻提供了低熱阻的熱傳機制，可在不增加電子設備溫度情況下，確保電子設備的正常運行，甚至提升其效能。將液體冷卻劑通道直接嵌入電子設備中，例如 3D 晶片堆疊設計，非常具有潛力。另外，Prof. Garimella 介紹許多熱管理新技術，如微流道(microchannels)、熱管(heat pipe)、蒸發冷卻(evaporation cooling)、電漿驅動(electrohydrodynamics, EHD)、離子風(ionic wind)、壓電風扇(piezoelectric fan)、多孔金屬架構(porous metal forms)、奈米芯結構(nanostructured wicking materials)、均溫板(vapor chamber)等。最後，Prof. Garimella 提出 MicroICE (microcooling for intensely concentrated electronics)方法，如**圖 2** 所示，傳統的熱管理為單向流道，目前已有多向流道，未來預期可朝分級流道進行設計，以達到高熱通量及低熱阻的目標。使用 HFE-7100 為冷卻液、質量流率 2100 $kg/m^2 \cdot s$ 條件下，升溫 20°C 時的散熱通量可以達到 400 W/cm^2，升溫 40°C 時的散熱通量可以達到 900 W/cm^2，升溫 45°C 時的散熱通量可以達到 1015 W/cm^2 並且可以移除局部熱點的熱通量高達 2600 W/cm^2，符合未來高熱通量及低熱阻的要求。

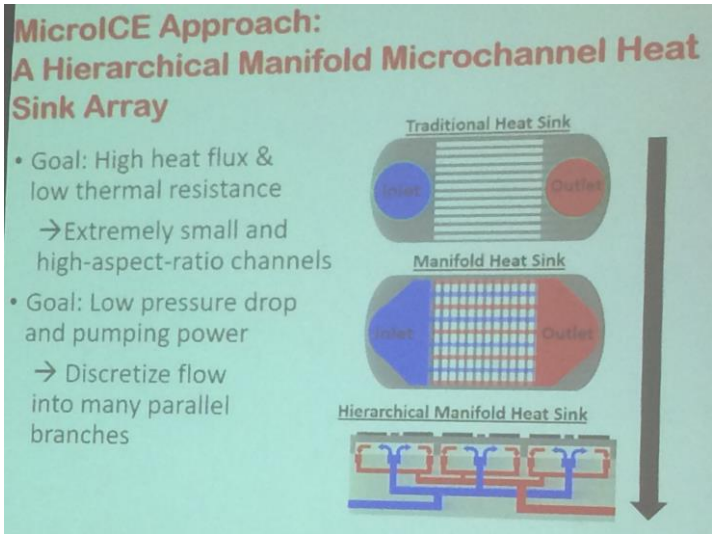

圖 2：主題演講時 Prof. Garimella 分享的 MicroICE 熱管理前瞻技術

第四場主題講題為 “Closed Carbon Cycle Economy”，講者 Prof. Roland Span 是德國 Ruhr 大學機械工程學院院長及熱力學主席。Prof. Roland Span 教授 1983~1988 年在 Ruhr-University Bochum (RUB)大學機械工程系就讀，1992 年獲得博士學位。曾在瑞士 Alstom 電力技術公司從事燃氣輪機相關研發工作，包括加濕式燃氣輪機和碳捕捉及封存(CCS, Carbon Capture & Storage)。2002 年擔任 University of Paderborn 熱力學與能源技術系主任。2006 年轉至 RUB 大學任教，擔任熱力學主席，領導了一個擁有約 25 名科學同事和 25 名研究生的研究所。Prof. Span 發表多篇被高度引用的科學論文，特別在熱力學性質的實驗和理論研究工作，及相應模型在能源技術中的應用模擬。他是機械工程學院院長，研究部閉路碳循環經濟研究部三位發言人之一，也是歐洲科學與藝術學院院士。

Prof. Span 指出，2015 在巴黎舉辦的 COP-21 會議中，與會代表們表達了二氧化碳減排減輕氣候變遷的政治意願，但社會民眾仍須一段很長的時間才能完全接受。如何完成這項任務？長遠來看，要解決人為溫室氣體排放的問題，必須透過整個社會和經濟體系的重組，才有機會達成封閉式碳循環社會。

碳使用是不可避免的，但是對環境的淨衝擊效應，可以透過全面考慮循環過程，來最大限度地減少。除了開發新技術之外，封閉型碳循環經濟還須有更廣泛的思考，已非單一學門可以解決的事情，跨學科合作一起努力是必要的。因此 2015 年 RUB 大學成立了閉路碳循環經濟研究系，進行工程、自然科學、人文科學和社會科學等跨學科領域研究人員的合作。低碳能源系統牽涉內容複雜，每個人的觀點不會相同，不同產業關心的面向也不一致；隨著全球化趨勢，國與國間的交互影響也不可避免；如何系統性量化與分析？如何取得世界各國的數據？如何擬定合適的政策？乃重要但艱難的課題。因此全面性的系統分析越來越重要，跨領域整合、跨國合作與數據交流，乃掌握未來的不二法門。

類似的，Applied Energy 期刊及 ICAE 系列研討會也一直在推動 UNiLAB，UNiLAB 即 Universal Laboratory 的縮寫，希望建立一個國際合作平台，結合全世界相關研究團體，共同合作，交換心得與數據，目前已成立多個 UNiLAB，歡迎全世界各研究單位加入，有興趣者可至以下網站https://www.scientistsclub.org/了解。

三、心　得

第九屆應用能源國際研討會(ICAE2017)，於 2017 年 8 月 21~24 日於英國卡地夫舉行；該會議每年舉辦一次，國際主辦單位為 Applied Energy 期刊。Applied Energy 為能源領域中最具聲望的國際期刊之一，其最新的影響因子(impact factor)高達 7.182，排名榮登 Cite Score 能源領域的榜首；在 Google Scholar 永續能源領域上盤據亞軍；在 ISI 工程類排名高居第 5 名，無不顯示該期刊的重要地位。ICAE 每年的會議均有全球數十個國家的專家學者與會，發表超過 500 篇以上的論文，乃能源領域國際學術交流的重要會議之一，因此 ICAE 系列研討會值得繼續參加。

本次參加研討會的感受之一，除了結合理論與實驗之外，大量的實驗與模擬數據宜進行系統性分析或優化設計，可讓研究成果更上層樓。例如 Ge et al.以多目標最適化評估橫向流熱交換管束，將相關 CFD 及基因演算法的分析結果，進一步以 TOPSIS (Technique for Order Preference by Similarity to Ideal Solution)法進行優化(如**圖 3)**，結果熱傳量提高 53.5%、同時壓損降低 1.27%。

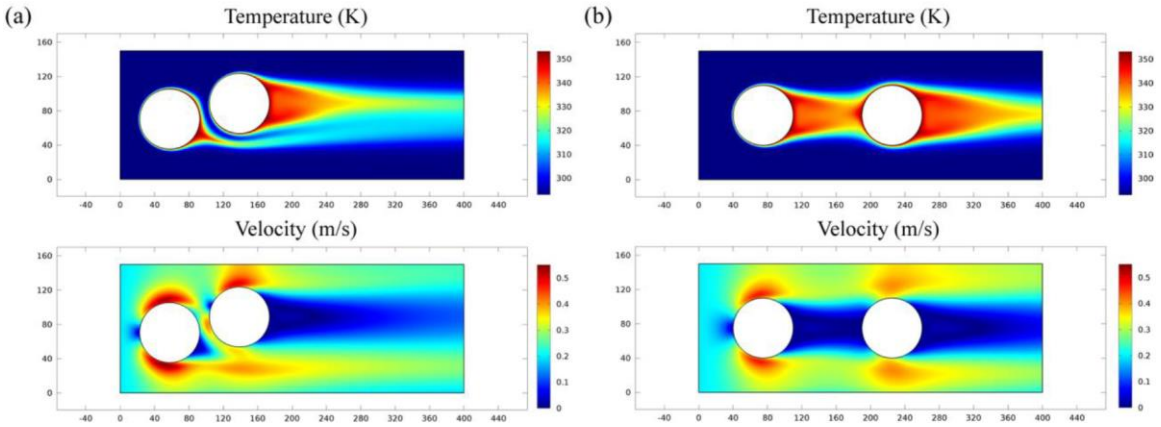

圖 3：橫向流管束排列之優化設計示意 (a)以 TOPSIS 優化設計例、(b)原始設計例

隨著人口都市化與土地取得越來越難，都市大樓越來越多，住商大樓建築節能也日趨重要，世界各國如此，我國也不例外。根據社團法人台灣環境資訊協會、環境資訊中心數據[4]，2016 年全台耗電創下歷年新高的 2,553 億度，比 2015 年增加 2.2%，其中五大用電部門的年增幅各為：工業+1.65%、運輸+1.04%、農業+0.10%、服務業+1.72%、住宅+5.46%，居首的

是激增 5.46%的「住宅」部門。若再看各部門的用電增長貢獻度，「住宅」再度以+45.3%比重超越「工業」+40.7%，「服務業」貢獻度亦高達+15.3%。換言之，2016 年每增加 100 度用電，約有 60 度用在住商(住宅&服務業)等建築生活空間上。另根據經濟部能源局辦公大樓能源查核統計分析，空調系統用電量佔建物總用電量 43% [5]。因此，空調系統用電乃節能上非常重要的一環。

本次會議中有一個研究，針對商業大樓分散式空調室外主機的散熱問題進行改善，題目為 Outdoor air thermal plume simulation of layer-based VRF air conditioners in high-rise buildings。其中，VRF 為 Variable Refrigerant Flow (可變冷媒流量)的英文縮寫，VRF 空調的市場，預計從 2017 年到 2021 年之間，每年以 9.24%的年複合成長率快速成長[6]。

一般建築設計基於美觀或易於設計，常將室外空調主機置於同一位置，上下層樓的室外主機處於同一線上(如**圖 4a** 所示)，該研究發現，下層的空調熱排氣，因熱空氣自然上浮的現象，會影響並提高上層空調的進氣溫度，導致效率下降與耗能增加。該文提出隔層排列的方法(如**圖 4b**)，即室外空調主機不要每層安裝，採用隔層安裝的排列方式，如此上層進氣溫度可以下降 22%，具有節能效果。

上述觀念頗值得參考，個人認為隔層安排可能會有土地使用權的爭議；或許可以考慮左右交錯方式，來降低空調室外機彼此的溫度干擾，提升空調節能效果。

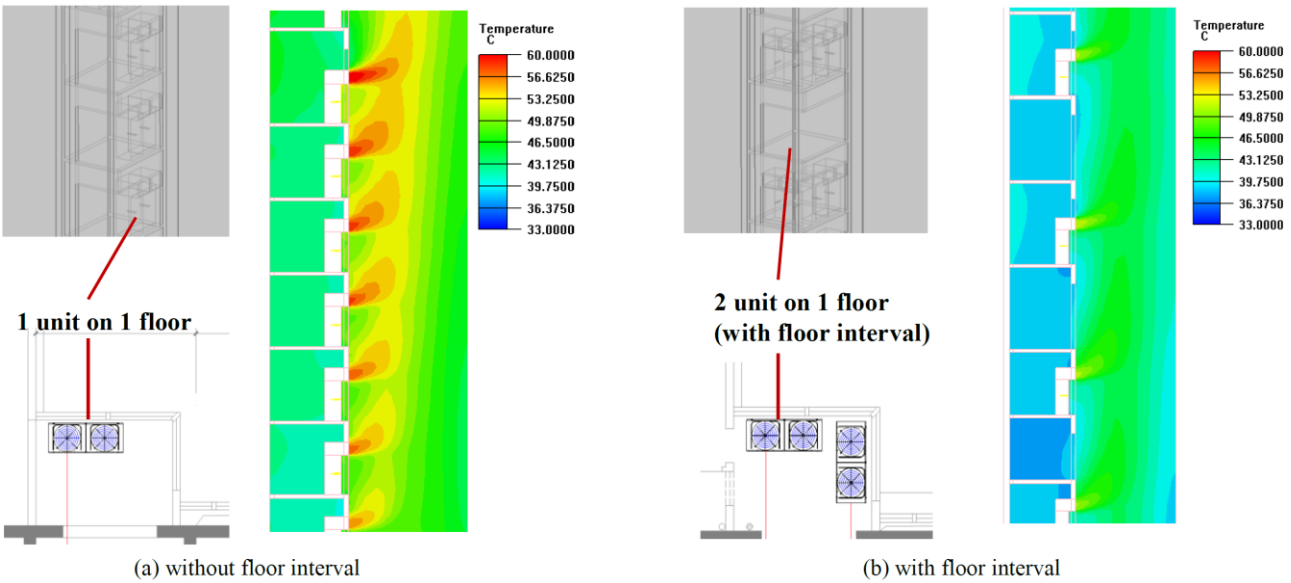

圖 4：大樓分散式室外空調節能設計及其溫度分布圖

(a)每層排列的傳統設計、(b)錯層排列的節能設計

根據臺灣電力公司網站揭露之資訊[7]，台灣位於菲律賓板塊與歐亞大陸板塊邊界，屬環太平洋火山帶，理論蘊藏量約 25,400 MW (百萬瓦)，其中宜蘭 7,400 MW，大屯地熱區 2,900 MW，花蓮及台東 15,100 MW。根據臺大地質系教授宋聖榮估計[8]，若將新北大屯火山群、宜蘭清水、土場、南投廬山、花蓮瑞穗、臺東霧鹿、金峰、金崙、高雄寶來、嘉義中崙、臺南關仔嶺等溫泉勝地的地熱發電潛能加總起來，擁有 33,640 MW 的地熱資源，約等於 24 座核四廠的發電量。科技部能源主軸計畫曾針對臺灣地熱潛能進行探勘調查[8]，臺灣地熱四大潛力區域(宜蘭平原、大屯火山群、花東地熱區、廬山地熱區)擁有 159,600 MW 的地熱發電潛能，若與美國 556,900 MW 的地熱發電潛能相比，台灣土地面積不到美國的百分之一，地熱潛力卻達到美國的 28.6%。雖然上述地熱發電潛能的數值落差頗大，台灣具有豐富地熱資源是個不爭的事實。另外，每個地熱位置的地質特性不同，開發難易度與風險差異頗大，使得地熱開發被歸屬於高風險投資，因此如何取得投資資金與降低投資風險至為關鍵，相關技術的發展也是必要的。

本次會議中有篇加拿大的研究 Intermittent Freezing Concept for Energy Saving in Artificial Ground Freezing Systems，探討人工地下冷凍(Artificial Ground Freezing, AGF)系統的節能控制方法。AGF 乃在地下適當處鑿井，在同心圓井內循環冷凍劑，將井外區域的水冷凍，來提高地下結構穩定化，或達到密封地下水之目的。AGF 已廣泛應用在寒帶國家的地下礦井、井沉降、隧道等工程，該文提出以間歇式冷凍劑循環的方式，取代傳統的持續循環模式，數值模擬的結果顯示可節能近 40%，AGF 及結果如**圖 5** 所示。

AGF 雖然在台灣不適用，吾人認為其原理可以類比於地熱換熱用途。地熱能利用若採用不抽水、單換熱的方法，鑿好井後，接著就在井管內循環工作流體，換熱量主要受限於地底地質熱傳性質，工作流體循環量並非越大越好，因為工作流體的壓損與輸送速率的平方成正比，且熱傳量主要受限在於地底地質偏低的熱傳係數(井外部)。換言之，適當的工作流體循環量與循環策略，可以減少所需動力(電力)，具有節能效益。

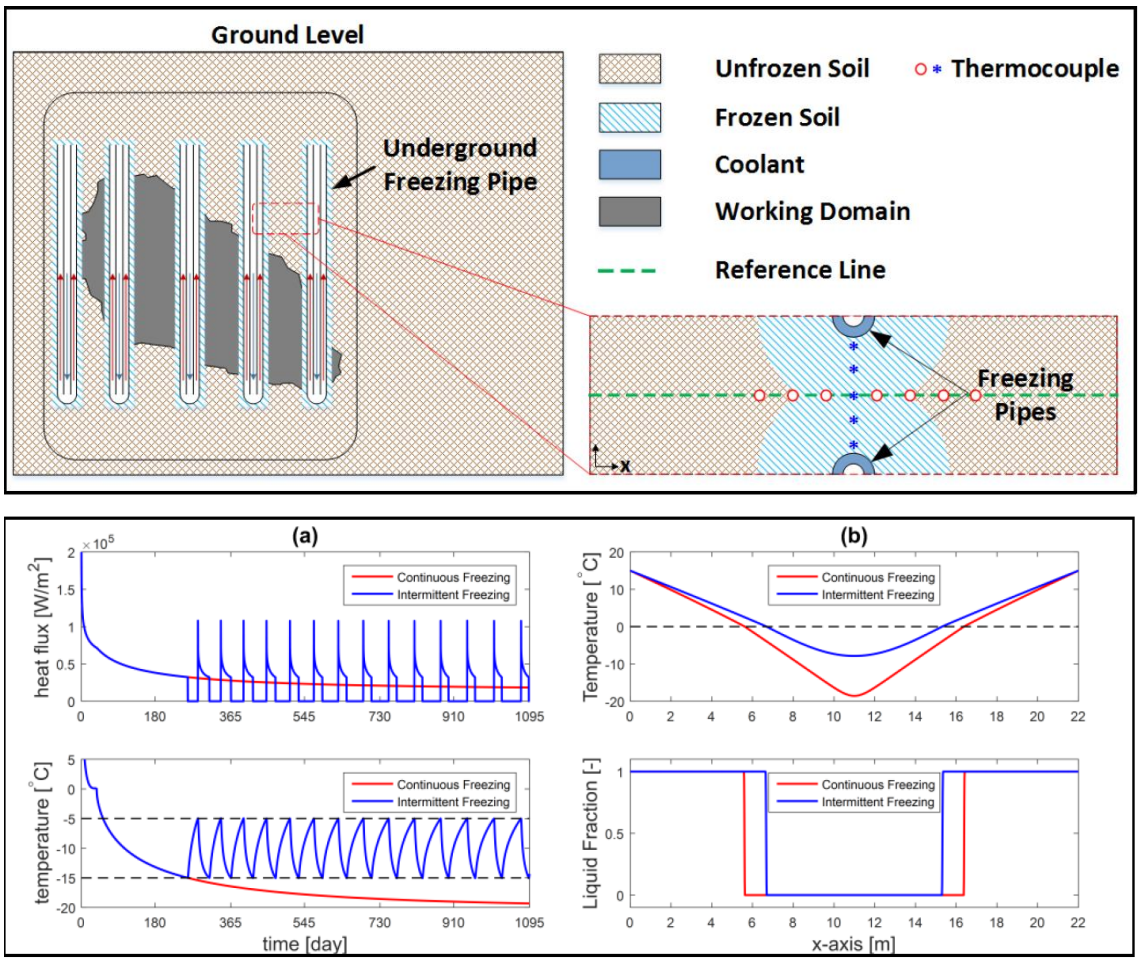

圖 5：人工地下冷凍及其節能操作策略

(上圖)人工地下冷凍方法示意、(下圖)間歇循環操作之節能結果

電子業毋庸置疑是目前台灣最重要的產業之一。根據國際半導體技術發展路線圖(International Technology Roadmap for Semiconductor, ITRS)在 2012 年的預測，積體電路上的功率密度可能在 2020 年時達到 100 W/cm^2 的數量級。在國防工業需求的微米與奈米高堆疊密度如雷達或高功率雷射的熱管理上，熱量密度甚至可能達到 1000 W/cm^2，因此先進電子技術已開始把熱管理整合納入設計考量。馬來西亞 Prof. Saw 發表一篇 Numerical analyses of the novel geometrically graded micro-channel heat sink 論文，提出分級微通道的新式散熱幾何(如**圖 6** 所示)，利用計算流體化學 CFD 模擬，結果顯示在功率 2000 W 或功率密度 222 W/cm^2 條件下，最高溫可由傳統未分級散熱的 105^{o}C 降至分級散熱的 71^{o}C，溫度差由 7.3^{o}C 降至 2.7^{o}C，顯示分級散熱的熱管理效果顯著，此方法值得借鏡與參考。

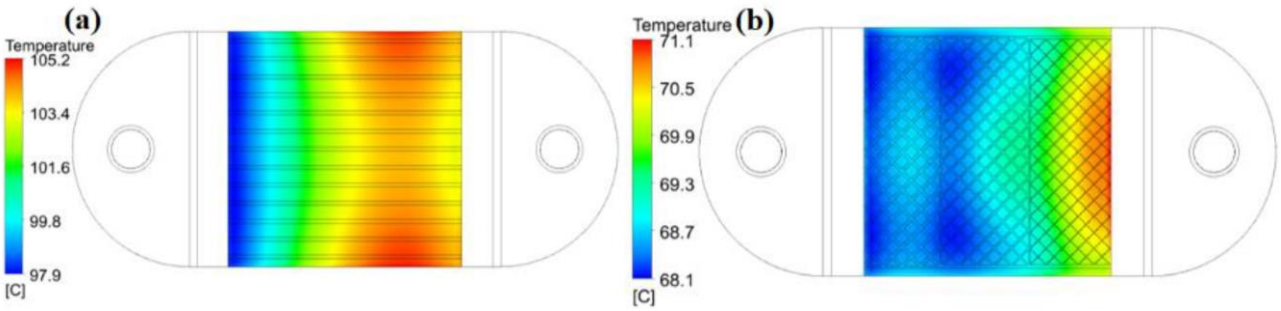

圖 6：電子散熱溫度分布圖 (a)傳統的直微通道、(b)新式的分級微通道

電動車自特斯拉(Tesla)公司 2009 年 3 月 26 日全電動豪華車 Model S 橫空出世後，引發全世界電動車熱潮。不到十年光景，電動車進程飛速，瑞典富豪汽車(Volvo)公司已宣布，2019 年起推出的所有新款汽車，都將是全電動車或油電混合車；英國預計 2030 年全面停止販售純石化燃料的新車，這些都是筆者(我想也應該是多數人)十年前難以意料的事，即使想的到還是對其進程之快速感到驚訝。台灣與特斯拉公司相當有淵源，曾有超過 1/4 零組件在台灣生產，包括電動車的心臟馬達、汽車中樞神經的電控系統等，都是出自台灣。現今，特斯拉電池管理系統線束的獨家供應商是我國貿聯公司，特斯拉電動車上數千顆 18650 鋰電池，還是必須仰賴我國的線材來串聯，凸顯我國電動車關鍵零件生產全球競爭力之事實。

鋰電池使用與充放電過程中都會放熱，使用時環境溫度的變異與差異，使得鋰電池組的熱管理至為重要。這也可由 2016 年三星手機鋰電池爆炸的全面回收事件，各大航空公司限制鋰電池託運，了解其嚴重性與重要性。特斯拉公司在鋰電池熱管理與安全管理方面確實有其獨到之處，多年下來，幾乎沒有主因於鋰電池的意外。電池是電動車的核心技術之一，鋰電池的熱管理，與其安全性及使用壽命有密切的關係，相關熱管理方法與技術的發展必然重要。本次會議中共有 7 篇關於鋰電池及其熱管理的研討：An echelon internal heating strategy for lithium-ion battery、Experimental study on thermal characteristics and temperature distribution of laminated lithium-ion power battery、Lithium battery parameter estimation via simplified single particle model、Modified electrochemical model for real-time estimation of lithium-ion concentration in battery、Numerical analyses on the mist cooling for lithium-ion battery、Optimal charge current of lithium ion battery、Study on the thermal interaction and heat dissipation of cylindrical lithium-ion battery cells 等，在 ICAE2017 研討會發表的論文，大部分會收錄在 Energy Procedia 期刊網站(https://www.journals.elsevier.com/energy-procedia)，並免費提供下載，有興趣的讀者可自行上網取得。

熱管(Heat Pipe)是一種具有快速傳熱特性的特殊裝置，熱傳係數可達數萬至數十萬 W/m·K，比優質熱傳材料如銅(k = ~400 W/m·K)與鋁(k = ~200 W/m·K)高出數十倍以上。熱管的應用廣泛，早期多在航太領域；後來成功運用於寒帶地區的熱交換以強化地質結構，如有名的美國阿拉斯加輸油管及大陸青藏鐵路等；目前已普遍用於電腦及手機等電子產品的散熱元件；未來朝向各式熱交換器、冷卻器、地熱引導等用途。

熱管的基本構造是個一內含流體的封閉管子或腔體，一端為加熱端(evaporation section)、另一端為冷凝端(condensation section)、視情況兩者之間有一段絕熱段(adiabatic section)。加熱端內部的流體受熱而蒸發，蒸發瞬間產生局部高壓，驅使氣體快速往另一端移動，氣體到達冷凝端時受冷而冷凝，冷凝液以重力、毛細力、或機械功回到受熱端，持續氣液二相變化及循環，也不斷地將熱能快速傳遞與交換，形成類似等溫熱傳的熱超導現象。

熱管熱交換器與傳統熱交換器相比，被視為未來工業餘熱回收的重要型式之一，具有以下優點：(1)傳熱係數高，用於熱回收時的回收率高；(2)傳熱量大，可在較小溫差下傳送較多熱量；(3)體積小、重量輕、結構緊密；(4)冷、熱流體相互隔絕，彼此不影響；(5)可提高壁溫，減輕低溫腐蝕；(6)適用溫度範圍廣；(7)熱流密度可調；(8)熱源不受限制；(9)無須電力或機械力；(10)構造簡單；(11)每支熱管獨立運作，大幅降低停機風險。

本次大會熱管(Heat Pipe)相關的文章共有三篇，題目分別為 A mathematical model for estimation of the maximum heat transfer capacity of tubular heat pipes with water and mesh wicks、Dynamic performance of loop heat pipes for cooling of electronics、Theoretical analysis of flat heat pipe with graded-porosity wick design，其中第一篇是筆者的論文(如**附錄二**)，另兩篇介紹於下。

Dynamic performance of loop heat pipes for cooling of electronics 一文為瑞典 Malardalen 大學的國際合作文章，作者們發展出一個以節點分析法及質能平衡的迴路型熱管(loop heat pipe)數學模型，迴路熱管及散熱實驗裝置如**圖 7** 所示。數學模型結果經證實與實驗相符後，作者們以此數學模型進行電腦中央處理器(CPU)熱動態模擬，**圖 8** 模擬結果顯示，CPU 表面溫度(T1)可以控制在 47.5^{o}C 至 73.1^{o}C，符合 CPU 溫度小於 80^{o}C 的通則規範。然而，若仔細觀察，其實 CPU 表面溫度(T1)尚未穩定，仍有緩步升溫的趨勢，一旦 CPU 持續滿載運轉，可能會有超溫風險。因此，吾人認為迴路熱管散熱可行，但該系統仍需再優化。

圖 9 為工作流體填充量對迴路熱管散熱性能的影響，**圖 9a** 為相同工作流體填充量條件下、改變蒸發腔體面積時的 CPU 最高溫度，可以發現蒸發面積太小或太大都不好，作者認為系統存在最佳填充率。會場上當面向作者請教，太小不佳可能是因為傳熱面積變小之故，太大變差可能是因為工作流體液位太低所致，但真實原因仍待進一步釐清。**圖 9b** 為相同工作流體填充率條件下、變動蒸發腔體面積時的 CPU 最高溫度，此處的填充率為 65%，**圖 9b** 的趨勢較**圖 9a** 單純，蒸發面積越大，CPU 最高溫度越低，散熱效果越好，乃合理的結果。整合**圖 9a** 及**圖 9b** 的結果，可以了解工作流體的填充率對迴路熱管的散熱性能影響至為關鍵。

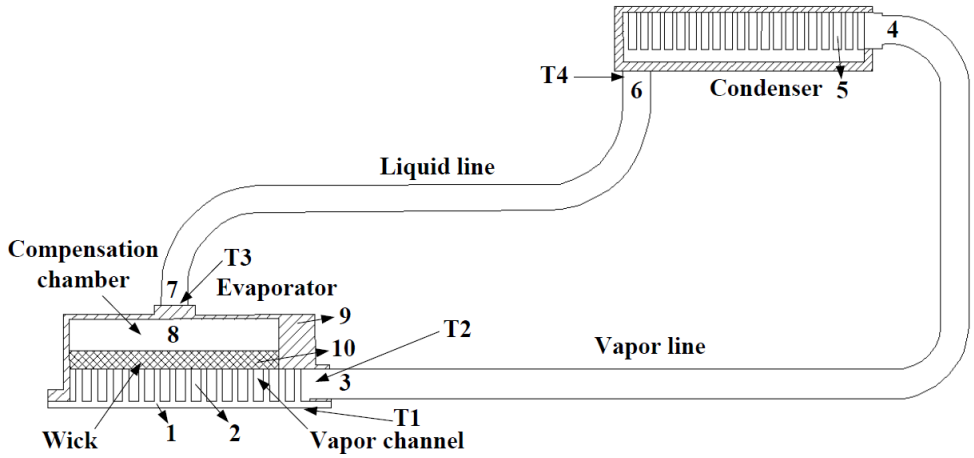

圖 7：電子散熱用迴路熱管示意

(1-Node of heating surface, 2-Node of vapor channel, 3-Node of evaporator outlet, 4-Node of condenser inlet, 5-Node of condenser, 6-Node of condenser outlet, 7-Node of compensation inlet, 8- Node of compensation, 9-Node of evaporator wall, 10- Node of wick)

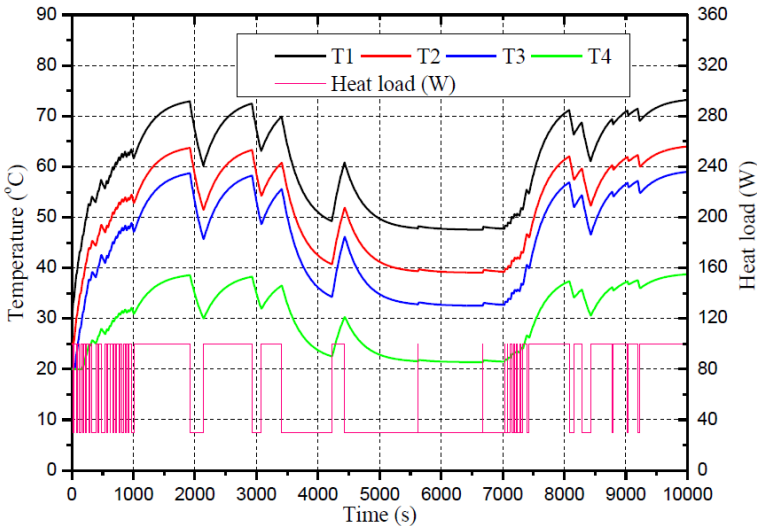

圖 8：動態 CPU 操作(熱)負載時，迴路熱管各點的溫度變化

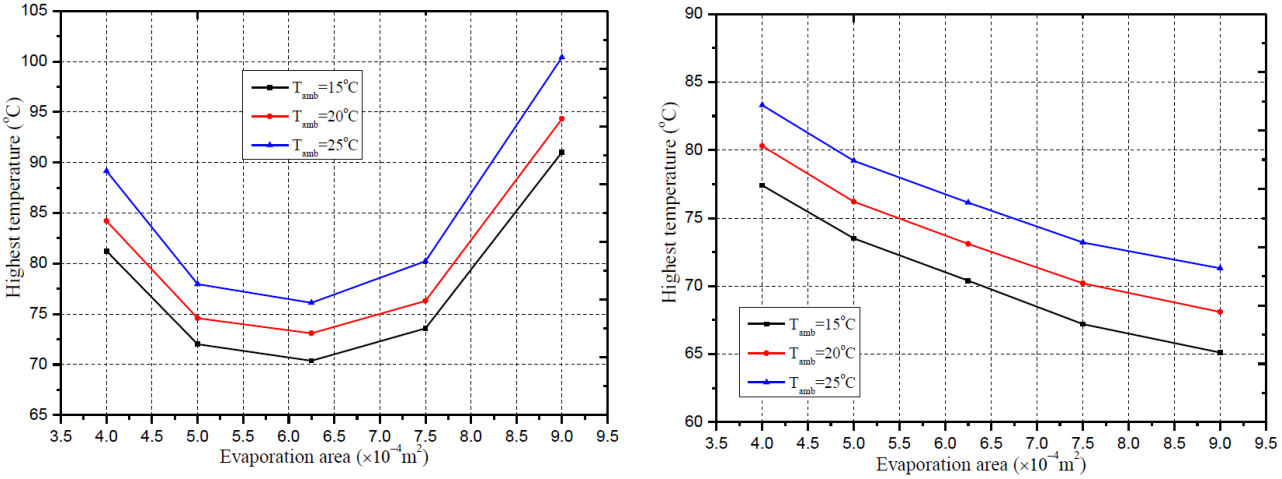

(a) The same amount working fluid　　(b) The same ratio of working fluid charging

圖 9：環路熱管蒸發面積對 CPU 最高溫度之影響

“Theoretical analysis of flat heat pipe with graded-porosity wick”一文以理論解析一維方向的槽型芯(groove wick)平板型熱管，提出兩種「漸擴式」槽型芯的新設計形式，如**圖 10b** 及**圖 10c** 所示；傳統的槽型芯可參見**圖 10a**，左側為蒸發段，右側為冷凝段。研究結果顯示，漸擴式設計的熱傳量較高，乃因為槽越小、蒸發腔體積越大，有利氣體流動，因此熱傳量獲得提升，此結果並不令人意外。然而實務上，漸擴式槽型芯在製作上較不容易，必須考量製作方法可行性與製作成本經濟性。

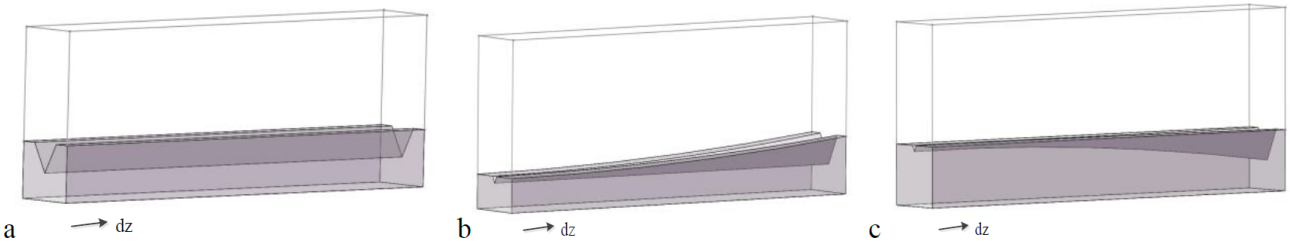

圖 10：槽型芯設計樣式 (a)傳統直線式、(b)向上漸擴式、(c)向下漸擴式

有機朗肯循環(Organic Rankine Cycle, ORC)是目前餘熱回收發電中被期待的關鍵技術之一。本次大會共有 13 篇 ORC 相關之論文發表，高篇數顯示 ORC 在國際間頗受重視。在本次會議上，研究內容主要在應用面，例如交通的柴油引擎廢熱回收發電、太陽熱能利用、微渦輪機汽電共生、空氣儲能、LNG 氣化程序、地熱應用等。從能源領域而言，包括交通節能、分散式電力、工業節能、建築節能、太陽光能、地熱能等。由上可知 ORC 應用領域相當廣泛。

以下針對本次研討會中發表的 ORC 文章摘要介紹。

在 ORC 柴油引擎廢熱回收方面，英國 Newcastle 大學發表一篇 “ORC units driven by engine waste heat –A simulation study”，本篇為純數值模擬，柴油引擎較小，引擎馬力約 10.5~12 kW、燃油噴量 2.8 L/h，ORC 工作流體為 R245fa。本篇考量兩種 ORC 熱源模式：(a)引擎廢熱直接供應 ORC 熱源、(b)以熱油循環提供 ORC 熱源，如**圖 11** 所示。**圖 12a** 顯示，引擎廢氣溫度與引擎負載有很大關係，溫度範圍介於 220~550^{o}C，不利後續 ORC 使用；若經過油熱交換，油溫可維持在穩定的 110^{o}C，較適合做為 ORC 之熱源，整體 ORC 熱利用可提高 5%~20% (**圖 12b**)。ORC 發電量亦隨負載變動，10%負載時僅約 0.14 kW，50%負載時約 0.62 kW，全負載時可達 1.25 kW；若扣除系統耗電量，ORC 淨發電量在 10%、50%、100%負載時各為 0.1、0.46、0.95 kW。

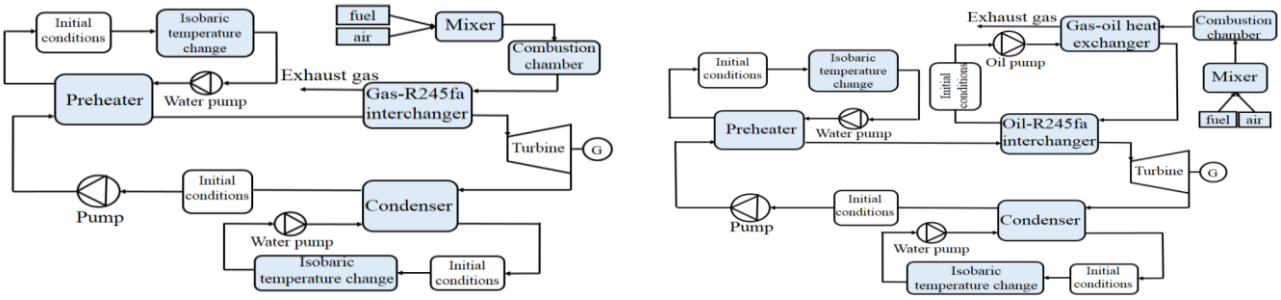

(a) 引擎廢熱直接供應 ORC 熱源　　**(b) 以熱油循環提供 ORC 熱源**

圖 11：柴油引擎廢熱 ORC 發電循環示意

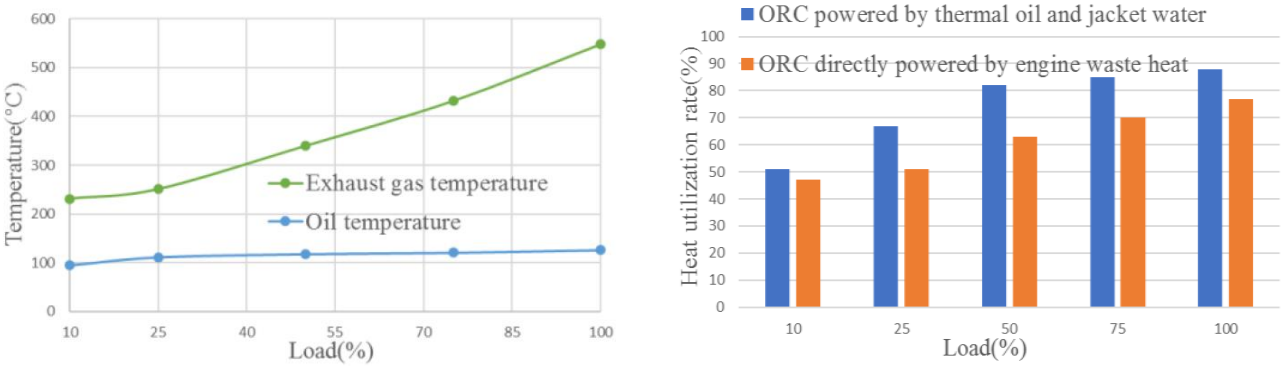

(a)引擎負載與溫度之關係　　**(b) ORC 發電量隨負載之關係**

圖 12：柴油引擎廢熱 ORC 發電模擬結果

由於車輛行駛為動態變化，ORC 能否跟上引擎動態變化？效能衝擊如何？並非靜態分析所能得知。這篇文章 “Dynamic simulation and analysis of Organic Rankine Cycle system for waste recovery from diesel engine”就是研究動態負載狀況下的 ORC 效能。在這篇研究中，選定的是大馬力 258.3 kW 的柴油引擎。研究中比較兩種熱源(a)引擎廢熱直接利用、(b)熱油循環，動態影響的差異約達 3 倍，熱油循環模式為較佳選擇。

跨臨界二氧化碳循環(CO_2 transcritical power cycle, CTPC)用於重型內燃機引擎廢熱回收發電，可見“Preliminary dynamic tests of a CO_2 transcritical power cycle for waste heat recovery from diesel engine”論文，作者們在實驗室建置一套 kW 級 CTPC 系統及其動態測試系統(**圖 13**)，實驗條件如下：柴油引擎轉速 1,100 rpm、引擎扭力 603 N·m、引擎馬力 69 kW、燃油噴量 14.96 kg/h、空氣量 348 kg/h、排氣溫度 465°C，引擎採用定閥門開度(CVO, constant valve opening)及定泵速度(CPS, constant pump speed)兩種操作方法。實驗與預測結果如**圖 14** 所示，CTPC 的最大淨電力輸出可達 1.34 kW_e，此時之熱電轉換效率約 3.54%。

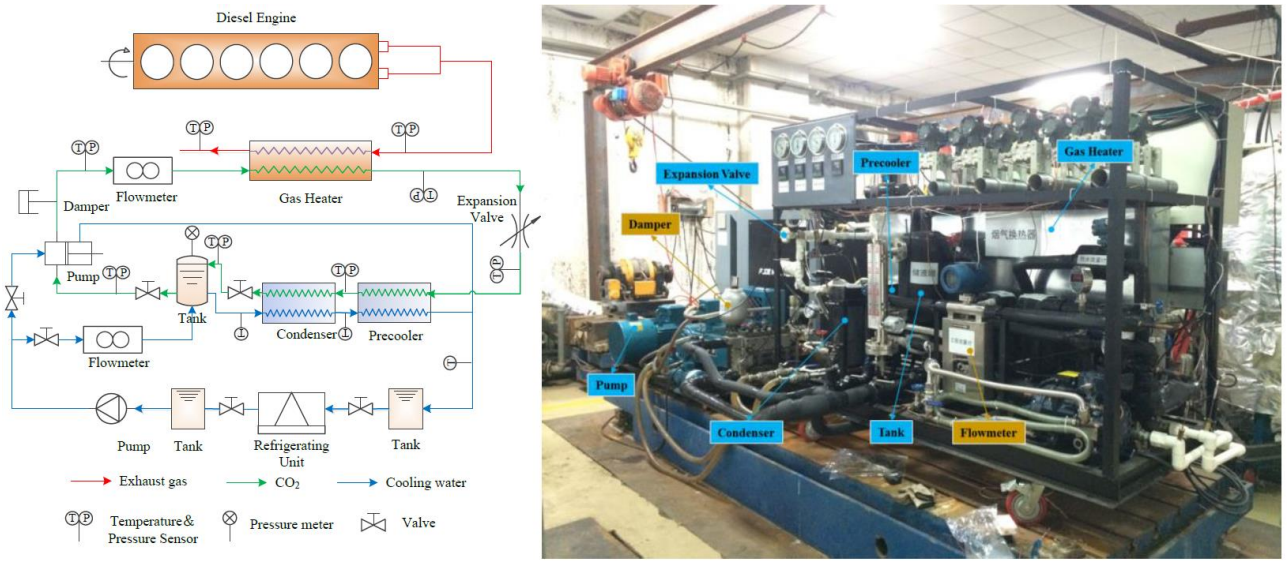

(a) **(b)**

圖 13：(a) kW 級跨臨界 CO_2 循環系統示意及(b)動態測試裝置照片

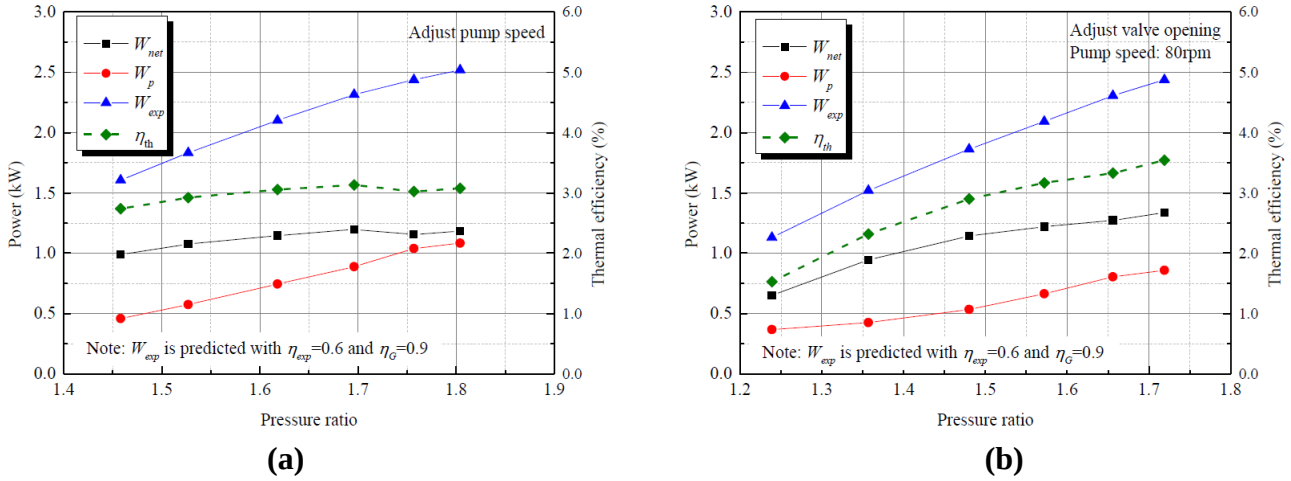

圖 14：跨臨界 CO_2 循環系統回收柴油引擎廢熱發電 (a) CVO、(b) CPS 操作模式

太陽熱電整合應用是個提升太陽光電效率的可行方向，“Clarifying the bifurcation point on design: A comparative analysis between solar-ORC and ORC-based solar-CCHP”提出 ORC-based solar-CCHP 優化系統(如**圖 15** 所示)，文中比較苯(benzene)、甲苯(toluene)、癸烷(decane)、八甲基環四矽氧烷(octamethylcyclotetrasiloxane)、六甲基二矽氧烷(hexamethyldisiloxane)等五種中溫工作流體，結論認為六甲基二矽氧烷為五者中之最佳選擇，熱電轉換效率可達 40.95%。

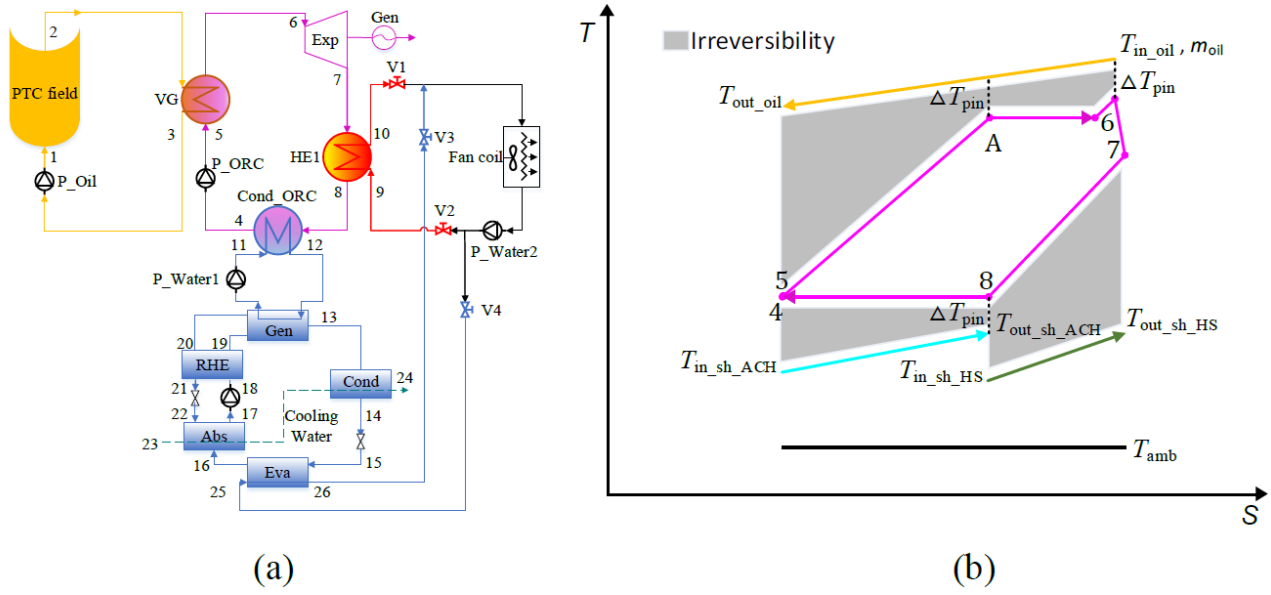

圖 15：ORC-based solar-CCHP 系統示意 (a)系統流程圖、(b)系統 T-S 圖

另有一篇太陽熱能 ORC 文章，是由義大利 Cioccolantia 學者所發表“Simulation analysis of an innovative micro-solar 2 kW_e Organic Rankine Cycle plant for residential applications”，研究中以模擬方法嘗試進行小型 ORC 與菲涅爾聚焦型透鏡太陽能集熱器(linear Fresnel lens collector)的系統整合，未來希望再整合相變材料(phase-change material, PCM)一同應用於建築節能上。模擬結果顯示，系統效能受環境條件影響，一年 12 個月會有變化，ORC 的年平均熱電效率 7.5%，淨發電效率為 4.5%，年變化率在±10%尚屬穩定。

ORC 結合微渦輪機(microturbine)方面，一般微渦輪機的排氣溫度仍有約 300^oC，很適合與 ORC 結合來提升效能或其他應用，本次研討會有兩篇此類的報告：(1)英國與中國合作的“An experimental investigation on a recuperative ORC system for electric power generation with low-grade thermal energy”，及(2)英國與義大利合作的 “Optimal sizing and operation of on-site combined heat and power systems for intermittent waste-heat recovery”。前篇文章透過實驗，實際量測採用一部 80 kW_e 微渦輪機作為汽電共生實驗裝置，這種規模的測試是少見的，因為不僅設備昂貴，實驗過程的燃料與電力成本也相當驚人，這是為何多數 ORC 文章多是以模擬為主，或是實驗室小規模實驗量測，像這種全尺寸的實驗實屬難得，其實驗數據頗值得參考。後篇文章乃在評估微渦輪機汽電共生系統串接 ORC 間歇操作的效能與成本，因為工業上有些製程，其加熱程序為間歇式，作者們思考，在起停爐中間若能加入 ORC，如此加熱源可以穩定操作，中間的熱能也可善加利用；不幸的是，評估後估計回本期達 21.3~23.7 年，恐怕難被業界接受。新技術要能成功，除了技術可行性之外，也要能符合業界接受度(成本經濟性)，否則最後不易實用化。

在 ORC 與空氣儲能方面，新加坡、義大利、比利時三國合作研究 “Preliminary assessment of waste heat recovery solution (ORC) to enhance the performance of liquid air energy storage system”。台灣是個島嶼，不像歐盟各國領土相連，電網容易跨國連接；隨著台灣未來再生能源發電比重的增加，儲能系統勢必越發重要。液態空氣儲能(liquid air energy storage, LAES)是儲能的可行技術之一，一般獨立式的 LAES 系統如**圖 16** 所示。該報告中提出兩種 ORC 與 LAES 的整合系統，如**圖 17** 所示。結果顯示，引入 ORC 可以提升 LAES 效率約 20%，回本期可以縮短 6%。

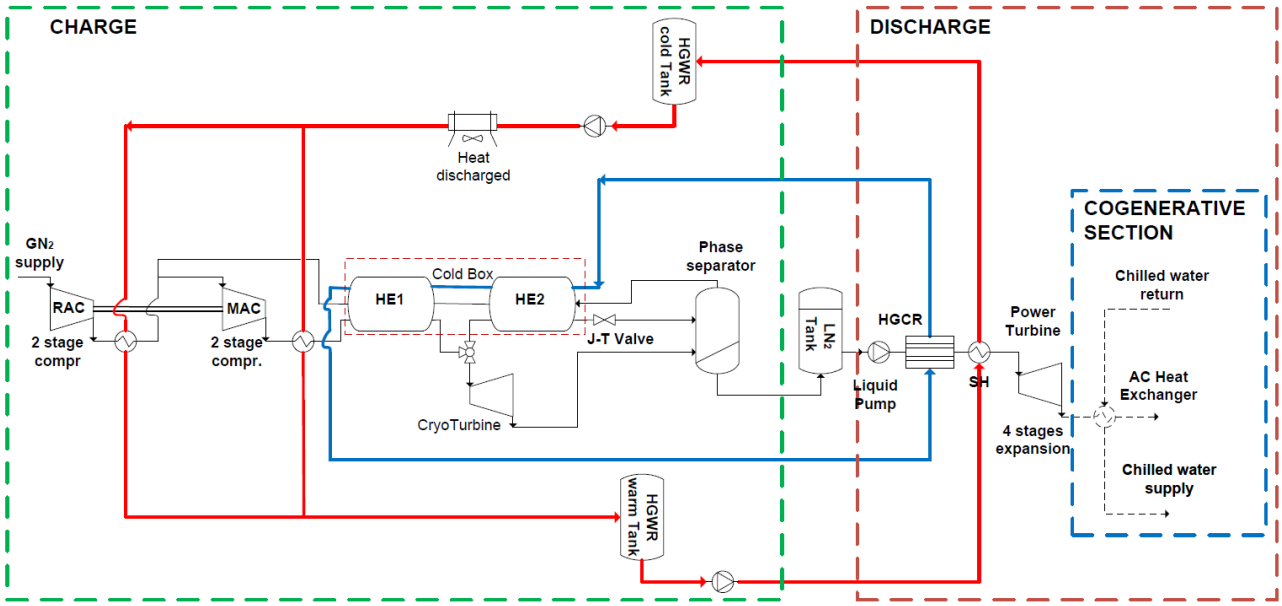

圖 16：液態空氣儲能(LAES)獨立式系統示意

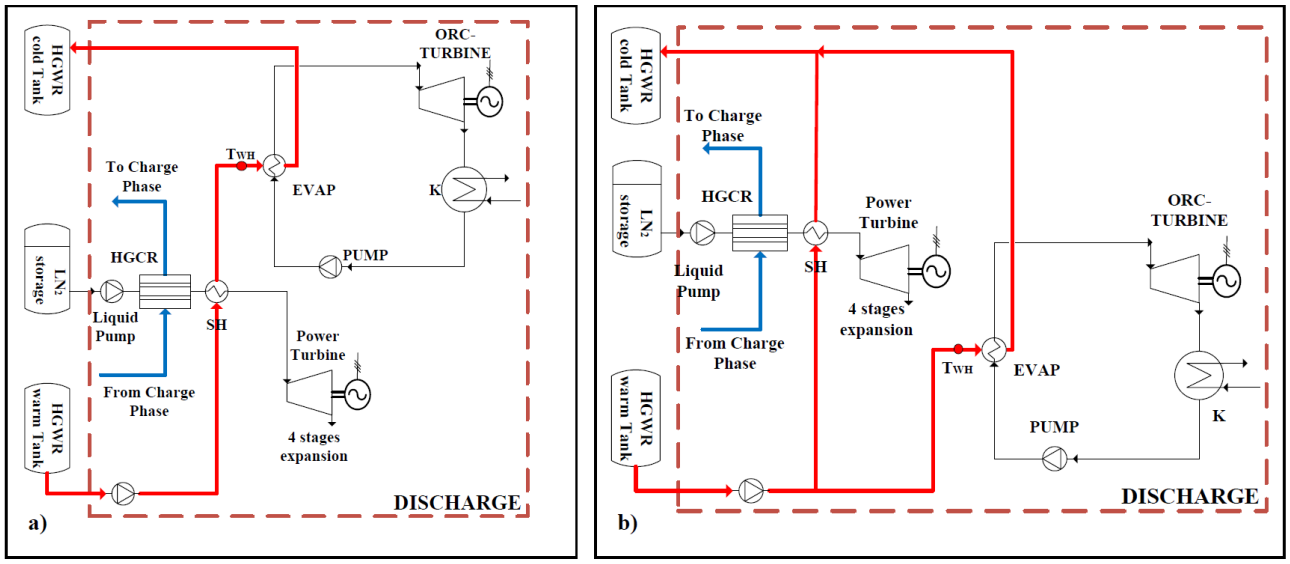

圖 17：兩種 ORC-LAES 整合系統示意

與上述壓縮空氣儲能應用原理類似，有一篇論文“Study of multi-stage condensation power generation systems for LNG cold energy recovery”，應用 ORC 於天然氣氣化站的能源回收與發電，因為 LNG 氣化程序的溫差很大，從 LNG 液化貯存溫度的約 –160°C 到室溫(或海水溫度)，此巨大溫差適合 ORC 發電，該文以程序模擬計算評估直接膨脹(DC)、ORC、複循環(CC)、兩階段冷凝 ORC (2ORC)、兩階段複循環(2CC)、三階段冷凝 ORC (3ORC)、三階段複循環(3CC)等 7 種技術。結果如**圖 18** 所示，就淨電力輸出而言，三階段冷凝 ORC 最高。若由電力生產成本(electricity production cost, EPC, $/kWh)觀點，複循環總是低於朗肯循環。但是淨電力輸

出量而言，朗肯循環高於複循環。

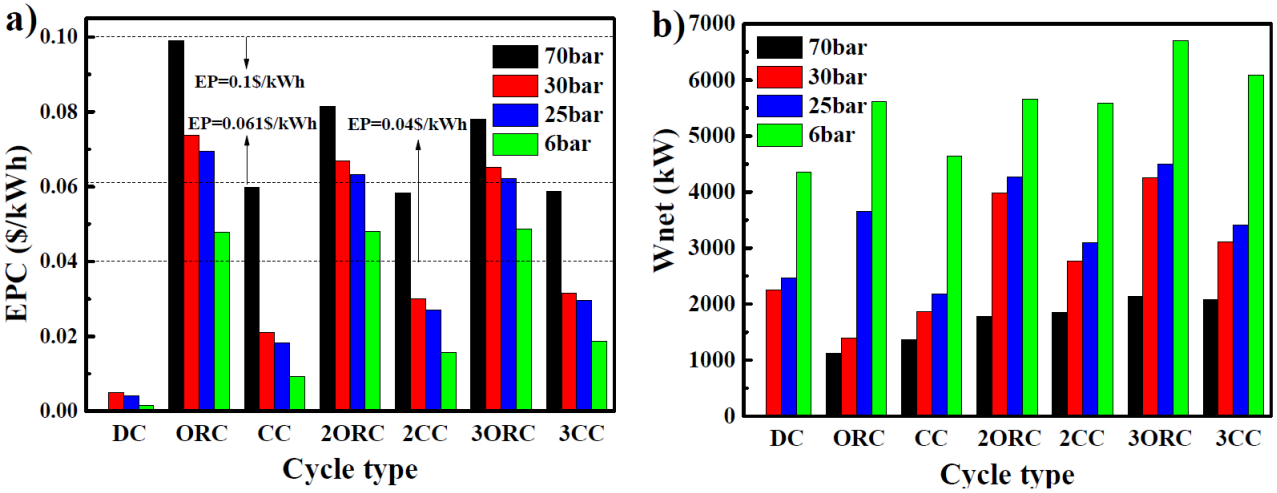

圖 18：液化天然氣氣化溫差發電七種技術比較 (a)發電電力生產成本、(b)淨發電量

在 ORC 地熱應用上，有一篇實務案例介紹 “A case study of an ORC geothermal power demonstration system under partial load conditions in Huabei Oilfield, China”，華北油田 1978 年開發至今已採集 98%的油藏，目前利用其地下高溫來產生熱流體，進行地熱能開發，裝設一部 500 kW_e的 ORC，工作流體為 R245a，設計參數詳見**表 5**，系統流程及主要設備照片請參見**圖 19**。運轉結果顯示，實際的發電量並無法達到設計值，大約只能達到約 30% (~150 kW_e)。現場操作經驗發現，系統效能的穩定性，會隨地熱水的變化而變動，因此如何獲得穩定的地熱水流量，相關技術與策略必須開發。**圖 20** 顯示，地熱 ORC 系統各組成的有效能損失(exergy loss)，以目前 43%負載條件而言，中間熱交換器(intermediate heat exchanger, IHE)佔了超過一半，為目前當下最值得投入改善之處。目前系統使用的熱交換為板式熱交換器，作者認為該型式的熱交換器良好，若系統設計時可以考量操作變動性，對操作彈性與系統效能會有幫助。

新技術發展，多先研究效率提升，開始應用與普及時，操作安全性就必須全面檢視。對於 ORC 而言，工作流體洩漏一定要盡可能避免與降低，因為除了降低效率之外，還會衍生安全問題。“Safe performance analysis of flammable mixture working fluid leakage in Organic Rankine Cycle”一文利用 CFD 模擬 ORC 工作流體洩漏後的擴散分布，並提出適當的檢測感應器安裝位置。

表 5：地熱 ORC 案例之設計參數

Parameters	Value	Parameters	Value
Ambient temperature (℃)	20.0	Isentropic efficiency of the turbine (%)	76
Inlet temperature of geothermal water (℃)	110.0	Mechanical efficiency (%)	96
Outlet temperature of geothermal water (℃)	85.7	Efficiency of the generator (%)	93
Inlet temperature of cooling water (℃)	20.0	Efficiency of the feeding pump (%)	70
Flow rate of geothermal water (m^3/h)	250	Efficiency of the water circulating pumps (%)	75
Mass flow rate of working fluid (t/h)	119	Pinch point temperature difference (℃)	6.0
Evaporation pressure (MPa)	0.819	Pressure drop in evaporator/condenser (Mpa)	0.050
Superheat at evaporator outlet (℃)	6.0	ORC thermal efficiency (%)	8.0
Condensation pressure (MPa)	0.187	Net power output (kW)	500

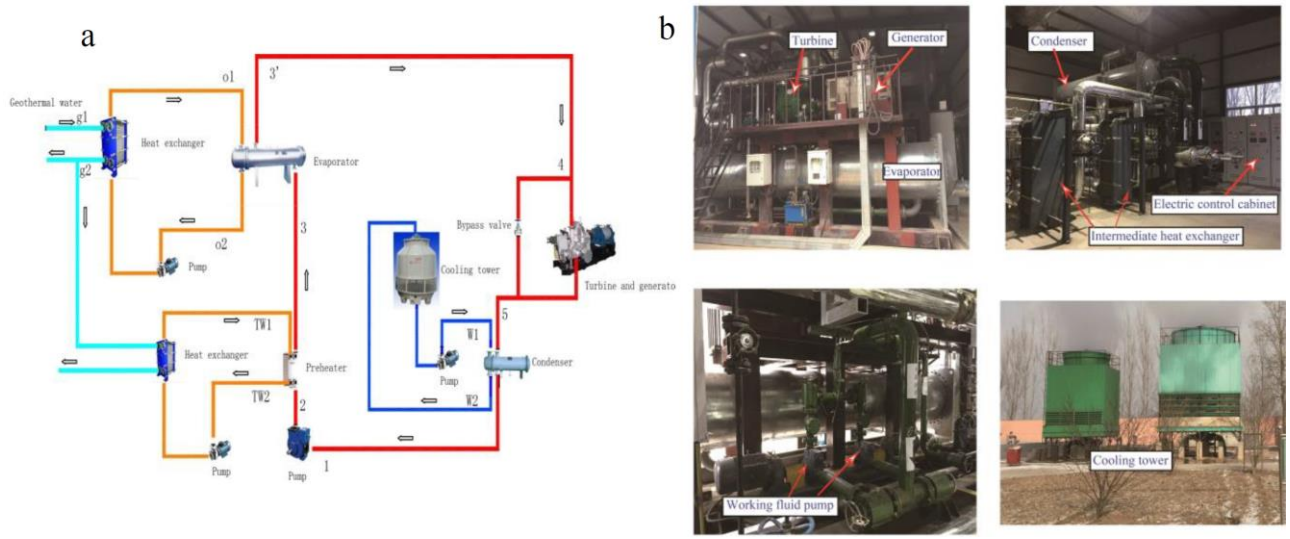

圖 19：地熱 ORC 案例之(a)系統流程示意及(b)相關照片

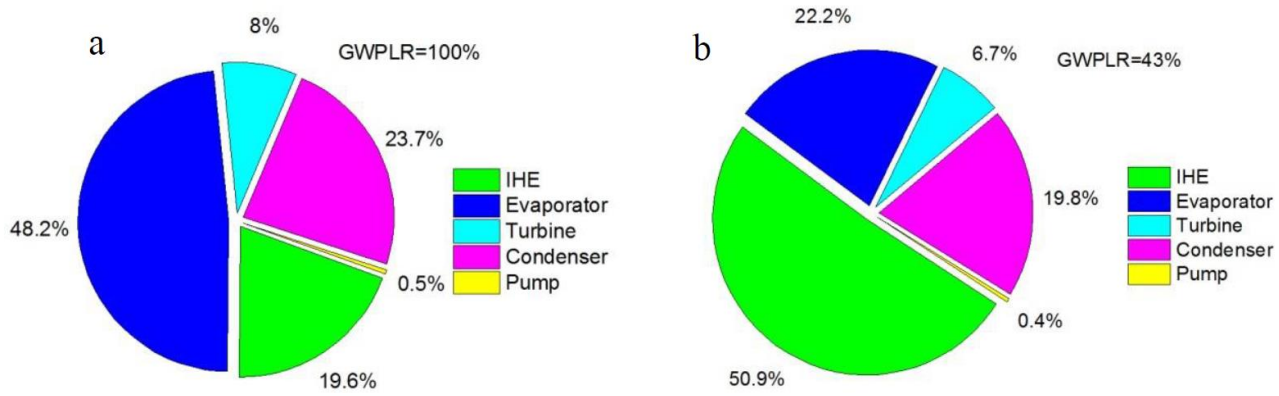

圖 20：地熱 ORC 案例之有效能損失組成 (a) 100%負載、(b) 43%負載

最後，筆者回程時，飛機上座位難得在窗邊，由卡地夫飛往阿姆斯特丹途中，恰巧看到離岸風機陣列，數量龐大，遂拿起手機拍了一張(**圖 21**)，可惜照相功能不佳，技術也不好，照片不太清楚甚是可惜。回國後查了飛機航線，比對風機數量，應該是 Greater Gabbard 風場，根據網路 Wikipedia 資訊(**表 6**)，共有 140 支 Siemens 風機，每支 3.6 MW，總裝置容量達 504 MW，容量因子(capacity factor)高達 42.2%。年發電量約 18.6 億度，是個發電效益非常高的一個風場。

根據台灣電力公司揭露資訊[9]，民國 105 年台電系統發電量共 2,258 億度，其中燃煤 36.9%、燃油 4.4%、燃氣 36%、汽電共生 2.6% (不含垃圾及沼氣)，再生能源占比為 5.1% (含水力及汽電共生中之垃圾及沼氣，風力佔 0.64%)，抽蓄水力 1.5%，核能 13.5%。換言之台灣 105 年風力總發電量約 14.47 億度，比英國單一個 Greater Gabbard 風場的發電量還少 30%。我國目前積極推動離岸風機，是個正確選擇，期許我國離岸風機再生電力早日落實。

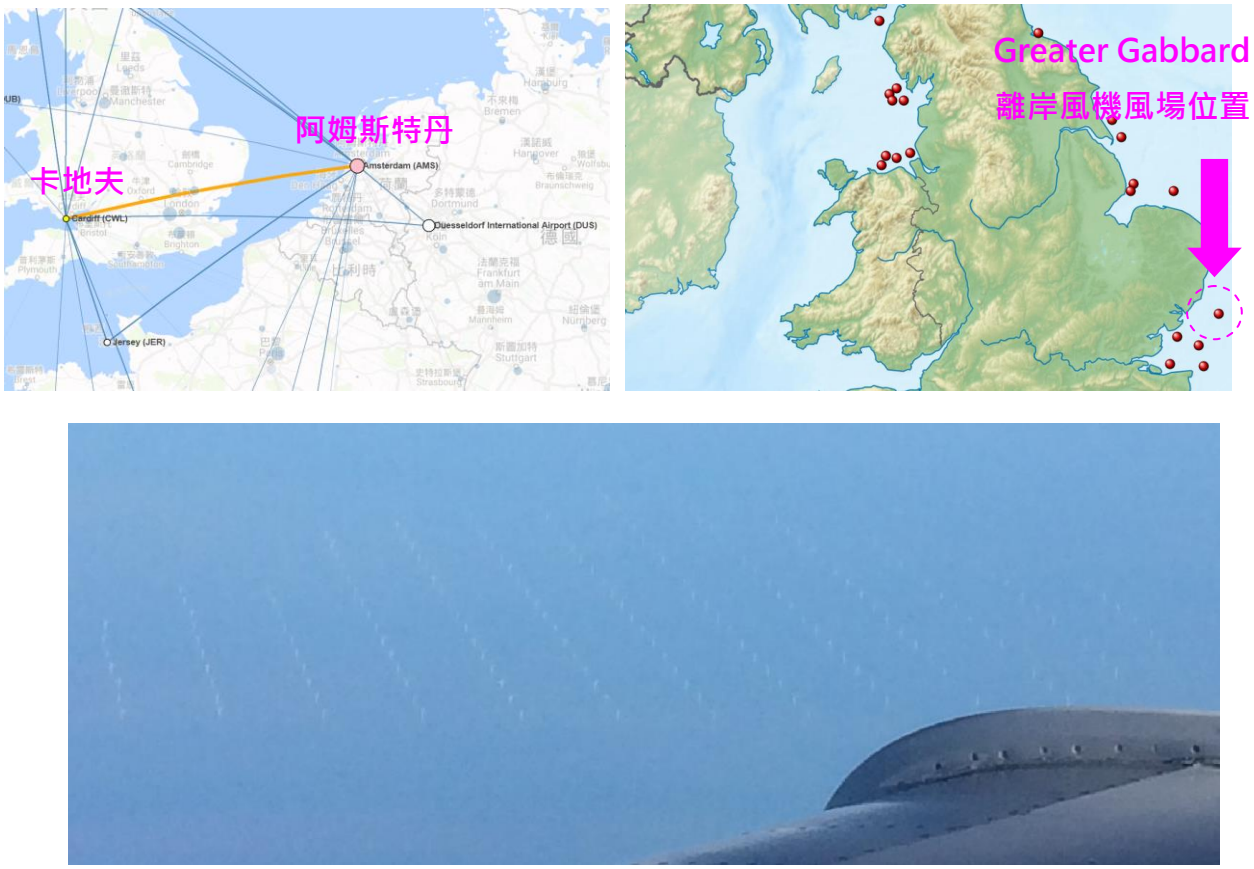

圖 21：筆者回程飛機途中巧見壯觀之英國離岸風機陣場

表 6：英國 Greater Gabbard 離岸風機風場資訊

風場名稱	Greater Gabbard
裝置容量	504 MW
風機	140 支 × Siemens SWT-3.6–107
位置	51°56′0″N　1°53′0″E
建置日期	2012 年 9 月
建造成本	£1500 百萬英鎊
容量效率	42.2%　(=實際發電量/裝置容量)
深度	20~32 m
離岸距離	23 km
擁有者	SSE Renewables
參考來源	Wikipedia, https://en.wikipedia.org/wiki/List_of_offshore_wind_farms_in_the_United_Kingdom

參考文獻

[1] 經濟部能源局，「讓能源充分發揮效益–工業廢熱回收」，能源報導，2014.09。

[2] Proceedings of the 9th International Conference on Applied Energy (ICAE2017), Cardiff, U.K., Aug. 21-24, 2017.

[3] https://www.inside.com.tw/2012/10/18/google-data-center-in-lenoir (下載日期 2017.09.01)。

[4] 社團法人台灣環境資訊協會、環境資訊中心，http://e-info.org.tw/node/205904 (下載日期 2017.09.02)。

[5] 臺灣電力公司，「建築物節約能源簡介」，2012。 http://info.taipower.com.tw/TaipowerWeb/upload/files/2/building_place_electricity.pdf

[6] "Global Variable Refrigerant Flow System Market 2017-2021," TechNavio (Infiniti Research Ltd.), 2017.06.21. http://www.giichinese.com.tw/report/infi518898-global-variable-refrigerant-flow-system-market.html

[7] 臺灣電力公司，http://www.taipower.com.tw/content/new_info/new_info-b36.aspx?LinkID=8 (下載日期 2017.09.09)。

[8] The News Lens 關鍵評論，https://www.thenewslens.com/article/52602 (下載日期 2017.09.05)。

[9] 臺灣電力公司，http://www.taipower.com.tw/content/new_info/new_info-c37.aspx (下載日期 2017.09.09)。

四、建　議　事　項

(一) 熱管內工作流體的填充率，對熱管傳熱量影響很大，填充率太低與太高均會降低傳熱量，最適填充量的預測方法值得研究。

(二) 有機朗肯循環是未來餘熱回收發電關鍵技術之一，ORC 可應用在許多領域或場合，微型且高效率 ORC 值得開發，以利工業餘熱回收及我國分散式電力之普及。

(三) 國家的長期電力規劃，必須鼓勵新技術及其發展，但不宜輕易放棄既有發電方法。研擬能源政策時，宜將民眾接受度、工業因應策略、執行方法、環保目標等納入考量。

(四) UNiLAB 國際合作平台乃 ICAE 系列研討所推動，跨國、跨領域一起合作，交換心得與數據，加速研發進程，值得我國與本所加入。ICAE 研討會值得繼續參加。

(五) 未來電子產品的熱管理要求日漸重要，以往單一學門或領域的獨立研究已難以滿足產業的現實需求，未來必須跨學門與領域合作，以系統全面思維發現及解決問題。

附錄一：發表論文 1

Available online at www.sciencedirect.com

ScienceDirect

Energy Procedia 00 (2017) 000–000

Energy Procedia

www.elsevier.com/locate/procedia

9th International Conference on Applied Energy, ICAE2017, 21-24 August 2017, Cardiff, UK

Perfluorocompounds emission control with thermal plasma torches

How Ming Lee*, Shiaw-Huei Chen

Physics Division, Institute of Nuclear Energy Research, 1000 Wenhua Rd. Jiaan Village, Longtan District, Taoyuan City 32546, Taiwan

Abstract

Perfluorocompounds (PFCs) have long lifetimes and high global-warming potentials. PFCs including CF_4, C_2F_6, C_3F_8, CHF_3, SF_6, NF_3, etc. are widely used in the electronic industries. Although the atmospheric concentrations of PFCs are currently much lower than CO_2, the annually increasing rate of CF_4 and SF_6 are 3.3 and 12 times higher than CO_2, respectively. The thermal plasma can offer an extremely high temperature stream for thermal decomposition of PFCs, and is regarded as a state-of-the-art technology for PFC emission control. In the study a thermal plasma torch is designed and experimentally tested for PFC abatements. Results show that PFC abatements are mainly determined by the plasma power, gas flow rate, and PFC's concentration. The effects of operational parameters are further evaluated by the multiple regressions and the sensitivity analysis. For CF_4, the most significant factor to the removal efficiency is the plasma power, and the flow rate plays a negative role. In addition, the most sensitivity factor to the energy efficiency goes to the CF_4 concentration. There is a trade-off between abatement efficiency and the energy efficiency. Further works on optimization of the thermal plasma system for PFC abatement is worth doing.

Peer-review under responsibility of the scientific committee of the 9th International Conference on Applied Energy.

Keywords: perfluorocompounds (PFCs), emission control technology, global warming, greenhouse gas (GHGs), thermal plasma.

1. Introduction

Perfluorocompounds (PFCs) have long lifetimes and high global-warming potentials. PFCs include CF_4, C_2F_6, C_3F_8, CHF_3, SF_6, and NF_3 that are extensively used as etching gases or chamber cleaning gases in semiconductor and LCD manufacturing industries. Table 1 lists PFCs' atmospheric concentrations and the increasing rate. The global warming potentials in time horizon of 100 years (GWP_{100}) of CO_2, CF_4 and SF_6 are 1, 6630 and 23500, respectively. The atmospheric lifetimes of CO_2, CF_4 and SF_6 are 30-95, 50000 and 3200 years, respectively. The rate of atmospheric concentration change of CO_2, CF_4 and SF_6 are 2.3 ppm/yr, 0.7 ppt/yr, and 0.27 ppt/yr, respectively. The annually increasing rate of CO_2, CF_4 and SF_6 are 0.27%/yr, 0.89%/yr, and 3.25%/yr, respectively. These facts reveal that comparing to CO_2, CF_4 and SF_6 have higher impact to the global warming, live many longer in the atmosphere, and faster increase rate. That is, PFCs emission control is deemed important.

Peer-review under responsibility of the scientific committee of the 9th International Conference on Applied Energy.

Global PFCs emissions are estimated at 0.95×10^{12} kg-CO_{2eq} in 2005 with an expected increase to 3.7×10^{12} kg-CO_{2eq} in 2050 if application of control technology remains at the current level [4]. Figure 1 shows the consumptions and emissions of PFCs based on the statistical data of the world semiconductor council (WSC). Among PFCs the highest usage was NF_3 of 69%, followed by CF_4 of 11%, and the rests were all lower than 5.4%. The most emissions were CF_4 (30%) and C_2F_6 (22%), NF_3 (16%) and SF_6 (11%). NF_3 is of a significantly high consumption and a relatively low emission, which is due to the lowest bond energy (N-F, 2.76 eV) among PFCs. On the contrary, CF_4 is of the strongest bond energy (C-F, 5.17 eV) and leads to its high emission. It is noted that eV stands for the electron volt and 1 eV equals to 1.6×10^{-19} J. For common hydrogen carbons, the C-C bond energy is 3.80 eV, which is higher than N-F and lower than C-F. This fact reveals that CF_4 is highly thermal stable and that is why CF_4 can sustain so long in the atmosphere (Table 1).

Table 1. Greenhouse gases and their atmospheric concentrations.

	CO_2	CH_4	N_2O	SF_6	CF_4	Ref.
GWP_{100}*	**1**	25.0	298	**23,500**	**6,630**	[1]
Atmospheric lifetime, yr	**30-95**	12.4	121	**3,200**	**50,000**	[2]
Pre-industrial atmospheric concentration	**280 ppm**	0.700 ppm	0.270 ppm	**0 ppt**	**40 ppt**	[2]
Atmospheric concentration (C)	**402 ppm**	1.823 ppm	0.327 ppm	**8.3 ppt**	**79 ppt**	[2]
Rate of concentration change (R)	**2.3 ppm/yr**	5 ppb/yr	0.8 ppb/yr	**0.27 ppt/yr**	**0.7 ppt/yr**	[2]
Annually increasing rate, (=R/C)	**0.57%/yr**	0.27%/yr	0.24%/yr	**3.25%/yr**	**0.89%/yr**	[this study]

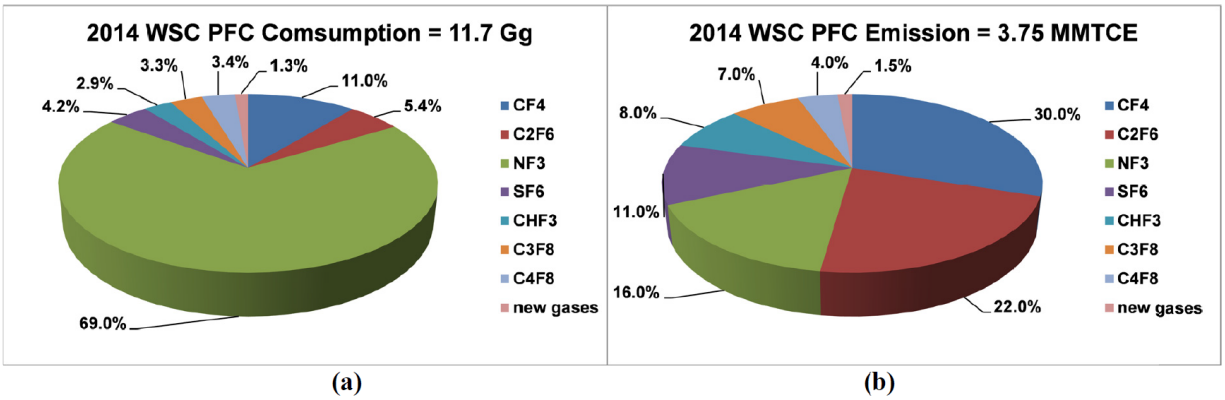

(a) (b)

Fig. 1. PFCs & SF_6 consumptions (a) and emissions (b) in the electronics industry. MMTCE stands for the million metric tons of carbon equivalent. Data from [3].

A thermal plasma torch can produce high enthalpy and extremely high temperature gases, and thus is successfully applied to decompose the highly thermal stable PFCs. The typical temperature is greater than 19000 K in the exit of a thermal plasma torch [5], and the average temperature ranging from 4000 to 6000 K depending on the plasma gas composition as well as the design of plasma torches. The plasma temperature is much greater than the combustion temperature, which is beneficial to PFCs thermal decomposition. In addition to thermal plasma abatement, there are other techniques also showing good PFCs abatement efficiencies. The advantages and disadvantages of PFC abatement technologies are summarized in Table 2. Considering both energy consumption reduction and emissions control [6], thermal plasma PFCs abatements override other abatement technologies due to the fast startup. In the study a thermal plasma torch is designed and extensively tested for PFC abatements at the Institute of Nuclear

Energy Research (INER). The effects of operational parameters are determined by experiments, multiple regressions, and sensitivity analysis.

Table 2. Advantages and disadvantages of PFC abatement technologies.

Types	Pressure	Advantages	Disadvantages
Thermal Oxidation	1.0 bar	1. DRE* > 99% 2. T >1200°C 3. Matured technique 4. Mid. cost, high maintains	1. Fuel gas (H_2/CH_4) cost high 2. Potential fire hazards 3. CF_4 DRE > 90%.
Thermal Catalysis	1.0 bar	1. DRE > 99% 2. Matured technique 3. 500 < T < 750°C 4. High cost, mid. Maintains	1. Aging and poisoning of catalyst 2. Used and wasted catalyst treatment 3. Can't handle SiH_4
RF / MW Plasma	Vacuum	1. DRE > 90% 2. Operated at low pressure 3. Local high temp., energy saving 4. Clean process (no electrode)	1. More byproducts COF_2, HCN, HF, SO_2, & CH_2F_2 2. Vacuum pump (HF) and EMI problems 3. High cost on RF/MW power supply 3. CF_4 DRE >85%
Non-Thermal Plasma	1.0 bar	1. DRE > 90% 2. Room temp. process 3. Energy saving 4. Mid cost, low Maintains (?)	1. Byproducts COF_2,CO, HF 2. CF_4 DRE >70% 3. Low flow rate 4. Still in developing stage
Thermal Plasma	1.0 bar	1. High DRE > 99.9% 2. Can operated at T >1200°C 3. Fast startup and no fuel gas 4. Mid cost, mid maintains (?)	1. Torch cathode life time too short 2. Strict demand on torch cooling 3. High cost on torch power supply

2. Experimental Setup

2.1. Thermal plasma system

Fig. 2 illustrates INER's thermal plasma PFCs abatement system, which is composed of a thermal plasma torch, a power supply for the plasma torch, a plasma mixing chamber, a reaction chamber, a quenching zone, a wet scrubber, a venting fan, and a monitoring & control unit. A well-type thermal plasma torch with copper as electrodes' material is used in the study. Two types of plasma mixing chambers including concurrent- and cross-flows are used in this study as showed in Fig. 3. Experimental results indicate that a vertical arrangement of plasma torch is better than a horizontal one, due to less SiO_2 deposition problem. The PFCs stream is first mixed with thermal plasmas stream in a mixing chamber. The mixing stream then flows into a PFC reaction chamber. The temperature of PFC streams is adjusted to a designed abatement temperature by the plasma power, where the designed abatement temperature is determined by the kind of PFC to be abated. In general, in the study, the abatement temperatures are set in the order of NF_3<CHF_3=C_2F_6=SF_6<CF_4. Since the plasma temperature is extremely high, a Venturi scrubber is installed at the exit of the reaction chamber, to cool down the temperature of gas streams as well as to avoid thermal damage of the whole abatement system. Downstream of the Venturi scrubber, a packing tower wet scrubber is installed for removal of acidic byproducts like HF, SO_2, HNO_3, etc. generated during previous PFC abatement processes.

The power of plasma torch is supplied by a DC high power supply with voltages ranging from 5 to 20 kW. For energy-saving, the plasma power adjusts automatically with signals of an optical emission spectrometer (OES). The plasma power is always turned on and set to the minimum in the idol operation mode. When OES measurement detects PFCs or other unwanted gases passing through the plasma chamber, the plasma power is automatically stepping up until concentrations of treated gases down to a setting ppm level. A calibration between OES signals and PFCs concentrations should be done in advance.

2.2. Experimental tests for PFCs abatement

In the study, it is experimentally tested for five kinds of PFCs including CF_4, CHF_3, C_2F_6, NF_3, and SF_6; three gas flow rates of 100, 200, and 300 SLPM (standard liter per minute); four plasma powers of 10, 12, 14, 16 kW; five PFC concentrations of 2000, 3000, 4000, 5000, 10000 ppmv; and with or without water addition.

A Fourier transform infrared spectroscopy (FTIR, Bruker, Vector 33, resolution 0.4 cm^{-1}) is used to on-line measurement of PFC concentrations. The characteristic wavelengths for determination of CF_4, CHF_3, C_2F_6, NF_3, and SF_6 concentrations are of 1281, 1150, 1249, 912, and 943 cm^{-1}, respectively.

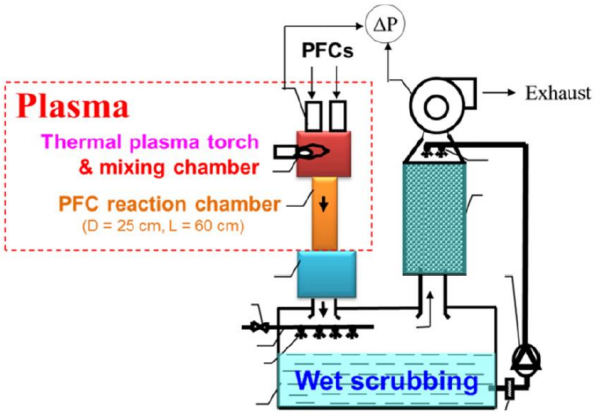

Fig. 2. Illustration of the thermal plasma PFC abatement system.

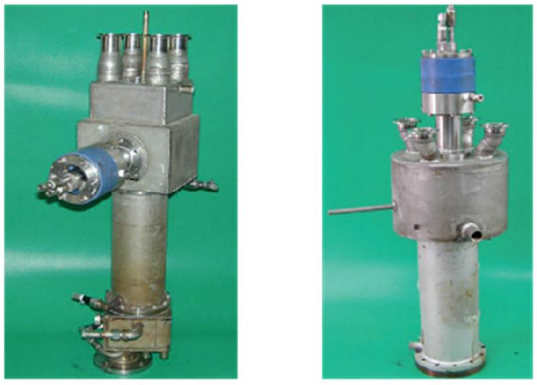

(a) (b)

Fig. 3. Photos of plasma abatement chamber, (a) the cross flow type; (b) the concurrent flow type.

3. Results and Discussion

Fig. 4 shows the FTIR absorption spectrum for PFCs abatements of C_2F_6, NF_3, CHF_3 and SF_6. The experimental conditions for each test are listed directly on the figures. The PFC signals in FTIR spectrum are significantly reduced once the plasmas are turned on. Main products observed in FTIR include CO_2, CF_4, SO_2F_2, and NO_2. CO_2 is come from the carbon of PFCs. CF_4 is generated in the C_2F_6 abatement. SO_2F_2 is observed during SF_6 abatement. NO_2 is an unwanted byproduct, which is commonly formed in an oxygen-containing thermal plasma environment.

Fig. 5 summaries the destruction and removal efficiencies (*DRE*) of five kinds of PFCs with thermal plasma system. It is easily to achieve 100% *DRE* for NF_3. CF_4 has the lowest *DRE* and is the most difficulty to be removed. The *DRE* is in the order of $NF_3 > C_2F_6 > CHF_3 > SF_6 >> CF_4$, which is same in [7]. The tendency is somewhat similar to the bond energy, such as N-F 2.76, S-F 3.30, C-C 3.80, C-H 4.39, C-F 5.17 eV, respectively. However, it is not yet clear for SF_6, which has a low bond energy, but is with a bad *DRE*.

For NF_3, C_2F_6, CHF_3, and CF_4, the higher the concentration, the better *DRE* can be achieved. However, again, SF_6 has a different tendency: the higher SF_6 concentration, the lower SF_6 *DRE* is observed.

To better understanding the relationship between the *DRE* and the flow rate (Q, in SLPM), the concentration (C, in ppm), and the plasma power (P, in kW), the multiple regression is adopted in the study. With the data shown in Fig. 5, the multiple regression for CF_4 *DRE* is,

$$DRE = 2.268215565\text{E-}5*C - 0.001829564724*Q + 0.04615450509*P + 0.0469977343 \quad (1)$$

The coefficient of determination (R^2) of Eq.1 is 0.686.

Similar, the multiple regression for CF_4 energy efficiency (*EE*) is,

$$EE = -0.1518101579*C - 1.455710521*Q - 24.72936395*P + 2160.228935 \quad (2)$$

The coefficient of determination of Eq.2 is 0.640. Where, *EE* is defined as the PFC molecules removed per eV. That is, both *DRE* and *EE* should be as high as better. And one can use above equations to achieve the *DRE* and *EE* by changing the plasma power (P) for a specific Q and C case.

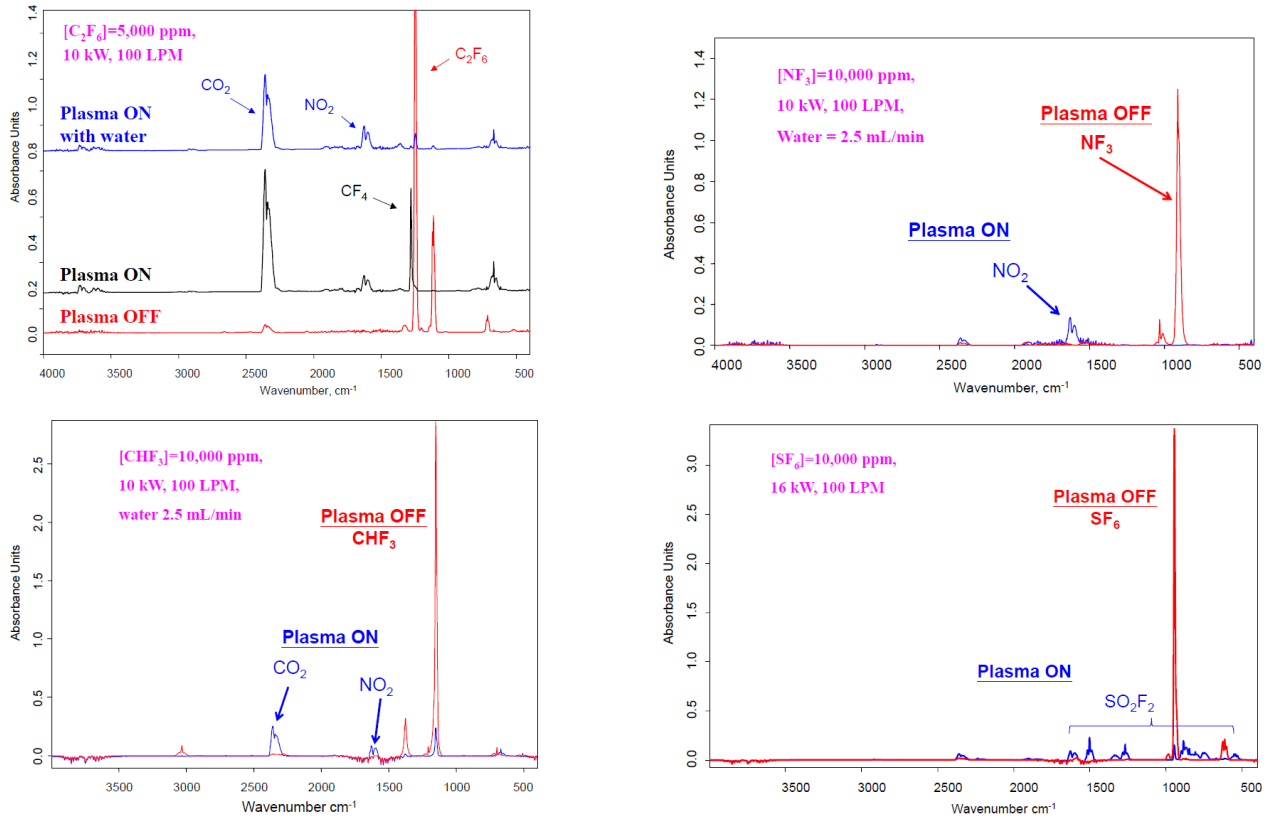

Fig. 4. FTIR absorption spectrum for abatement of C_2F_6, NF_3, CHF_3 and SF_6.

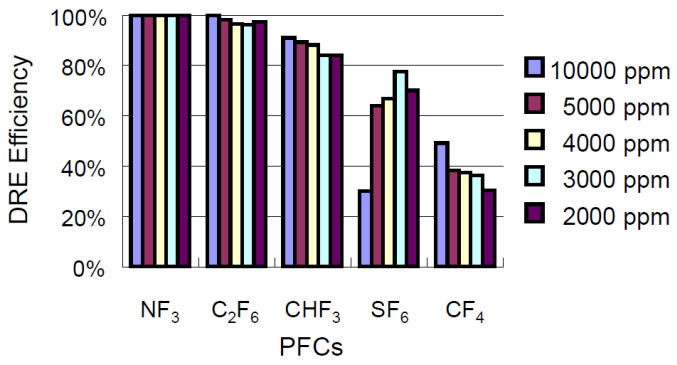

Fig. 5. Destruction and removal efficiencies (*DRE*) of five kinds of PFCs with thermal plasma torch.

Moreover, using Eqs. 1 and 2, the sensitivity analysis for PFCs abatement can be conducted. Figs. 6a and 6b plots results of the sensitivity analysis for *DRE* and *EE*, respectively. The base case is at the condition of Q_0=200 SLPM, P_0=13 kW, C_0=$[CF_4]_0$=5000 ppm. For DRE_{CF4}, it is clear that the most significant factor is the plasma power, and the flowrate plays a negative role. For EE_{CF4}, the most significant goes to the CF_4 concentration, which is different from DRE_{CF4}. An optimum design and/or operational condition by using the Eqs.1 and 2 as well as the sensitivity analysis are currently undergoing.

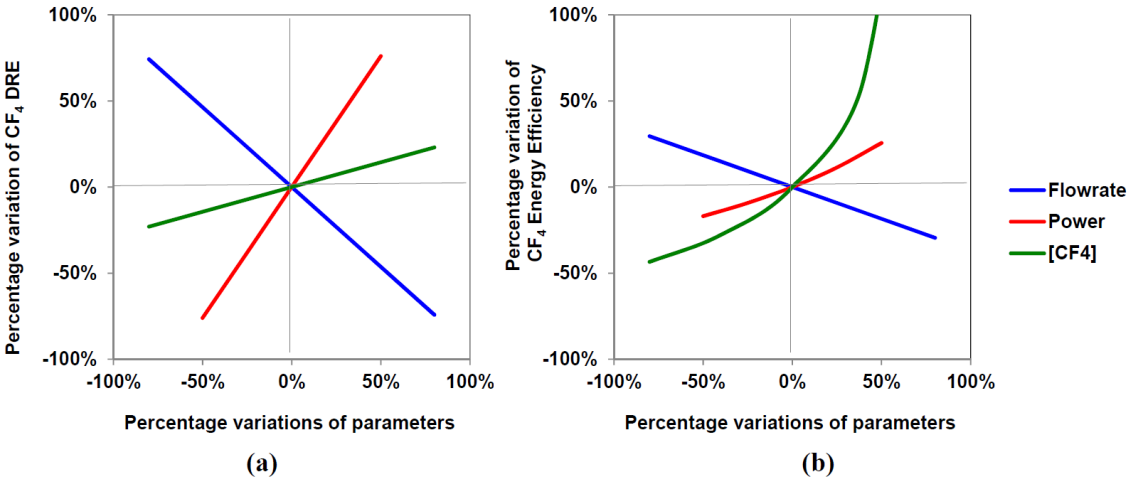

Fig. 6. Sensitivity analysis for CF_4 abatements, (a) the destruction and removal efficiency, *DRE*; (b) the energy efficiency, *EE*.

4. Conclusion and Suggestions

A thermal plasma system for PFC abatement has been developed in the study. Experimental results indicate that PFC abatements are mainly determined by the plasma power, gas flow rate, and PFC's concentration. Results of the multiple regressions and the sensitivity analysis reveal that the most significant factor to the CF_4 removal efficiency is the plasma power, and the flow rate plays a negative role. The most sensitivity factor to the CF_4 energy efficiency goes to the CF_4 concentration. There is a trade-off between abatement efficiency and the energy efficiency.

Some suggestions are also listed. (1) Mixing of the plasma stream and PFC stream plays a significant role to PFC abatement. (2) Kinetic data on PFC reactions at high temperatures are absent at present time. This leads to a difficulty in simulation as well as system optimization. Scientific research on this topic should be of contribution. (3) NOx is an unwanted byproduct in thermal plasma processes, and needs to be minimized. (4) Further works on optimization of the thermal plasma system for PFC abatement is worth doing.

Acknowledgements

Fund is from MOST 105-3111-Y-042A-070.

References

[1] IPCC, 2014: Climate Change 2014: Synthesis Report. Contribution of Working Groups I, II and III to the Fifth Assessment Report of the Intergovernmental Panel on Climate Change [Core Writing Team, R.K. Pachauri and L.A. Meyer (eds.)]. IPCC, Geneva, Switzerland.
[2] U.S. EPA, "Inventory of U.S. Greenhouse Gas Emissions and Sinks: 1990–2014," April 15, 2016.
[3] IPCC, 2016: "Industrial Processes and Product Use (IPPU)," Lesotho, Maseru, 14-18 March 2016.
[4] Purohit P. and L. Höglund-Isaksson: Atmos. Chem. Phys. Discuss., (2016).
[5] Chen, J.-S.; "Numerical simulations of well-type plasma torch," INER report #2933, Taiwan, 2004. *(in Chinese)*
[6] Neuber A. and M. Kranz: SEMICON Europa2015, (October 8, 2015).
[7] Beu, L. et al., "Current State of Technology: Perfluorocompound (PFC) Emissions Reduction," Technology Transfer # 98053508A-TR, International SEMATECH, June 2, 1998, p.47.

附錄二：發表論文 2

Available online at www.sciencedirect.com

ScienceDirect

Energy Procedia 00 (2017) 000–000

Energy Procedia

www.elsevier.com/locate/procedia

9th International Conference on Applied Energy, ICAE2017, 21-24 August 2017, Cardiff, UK

A mathematical model for estimation of the maximum heat transfer capacity of tubular heat pipes with water and mesh wicks

How Ming Lee*, Heng-Yi Li

Physics Division, Institute of Nuclear Energy Research, 1000 Wenhua Rd. Jiaan Village, Longtan District, Taoyuan City 32546, Taiwan

Abstract

Heat pipes are unique in their extremely high thermal conductivity and have high potential applications in the fields of heat recovery and renewable energy. The maximum heat transfer capacity of a heat pipe is determined by viscous, sonic, capillary, entrainment, and boiling limitations. There are dozens factors affecting the maximum capacity, for instance, the size of heat pipes, the capillary structure, the working fluids, and the operating condition. It would be difficult to design a high capacity heat pipe without a computational-aided tool. In this paper, a simple mathematical model is presented for quick estimation of the maximum heat transfer capacity of tubular water heat pipes with mesh wicks. The model prediction agrees well with other literatures and experimental data. To better understanding of heat pipes, with the model, a case study of a 2 meter long heat pipe for air-to-air heat exchanger application was performed. The influence of the evaporation temperature, the inclination angle, the mesh number, and the mesh layer on the maximum heat transfer capacity (Q_{max}) was analyzed. Results showed that their trends were nonmonotonic, and highly depending on the evaporation temperature. The simple mathematical model could serve as a handy tool for quick evaluation of Q_{max} as well as for speedup of a heat pipe design.

Peer-review under responsibility of the scientific committee of the 9th International Conference on Applied Energy.

Keywords: heat pipe, heat transfer limitation, maximum heat transfer capacity, air-to-air heat exchanger.

1. Introduction

The heat pipe is an excellent thermal conduction device with extremely high thermal conductivity. Heat pipes are widely used in the fields of aerospace, electronics cooling, heat exchanger, solar heat, geothermal, etc.

The R&Ds and applications of heat pipes are getting wider and wider. There are more than 130 heat pipes-related papers have been published on *Energy Procedia* in the past four years [1], and more than 8 technical review papers [2-9] last year in 2016. Institute of Nuclear Energy Research (INER) has started heat pipe R&Ds since 2014 [10-11], and high temperature heat pipe [12]. INER is now capable of manufacturing tubular heat pipes composed of copper, stainless steels, aluminum, or titanium, and with a set of working fluids like water, ammonia, ethanol, dowtherm or sodium. The lowest thermal resistance could achieve 0.07 K/W at a specific testing condition. To enhance the anti-

Peer-review under responsibility of the scientific committee of the 9th International Conference on Applied Energy.

corrosion ability as well as to widen applications of heat pipes, a thin film composed of TiN, CrC, or NiCr was coated on the outer surface of heat pipes [10].

Heat pipes have an extremely high thermal conductivity. The maximum heat transfer capacity of a heat pipe is determined by viscous limitation, sonic limitation, capillary limitation, entrainment limitation, and boiling limitation. There are dozens factors affecting the maximum capacity, for instance, the size of heat pipes, the capillary structure, the working fluids, and the operating condition. It would be difficult to design a high capacity heat pipe without a computational-aided tool. In this paper, a simple mathematical model is presented for quick estimation of the maximum heat transfer capacity of tubular water heat pipes with mesh wicks. In addition, a case study of a 2 m long heat pipe was performed to better understanding of heat pipes especially for the air-to-air heat exchanger applications.

2. Simple Mathematical Model of the Maximum Heat Transfer Capacity of Heat Pipes

2.1. Formulas of the maximum heat transfer capacity of heat pipes

The maximum heat transfer capacity of heat pipes had been well developed for decades. The maximum heat transfer capacity is regulated by five major limitations, i.e., viscous limitation, sonic limitation, capillary limitation, entrainment limitation and boiling limitation. Many empirical formulas of aforementioned limitations had been deduced, and can be found in textbooks and/or handbooks. However, the accuracy of the formulas is doubtful, because some errors and incompletions were found. It is especially confusing to a beginner in the field of heat pipes, like authors of this paper. Table 1 summarizes the five limitations. It is clearly observed that (1) different formulas are used in different literatures, (2) inconsistency in nomenclatures, and (3) incompletions of formulas. And even worse is that errors are found, for instance, the unit of all the limitations should be "W," but the unit of viscous limitation in [15] is "W/m^3" and the unit of boiling limitation in [14] is "W/m^2."

After examinations, authors recommend the formulas in [16] are fairly trustable. For simplicity, this study adopts the formula of capillary limitation in [15], because the formula of capillary limitation in [16] is relatively complicated and it cannot be directly used until consideration of Reynolds number and Mach number [16].

Table 1. Formulas of the heat transfer limitations of heat pipes.

Limitations	[13]	[14]	[15]	[16]	This study
Viscous	$Q_{vp}=\frac{\pi r_v^4 h_{fg}\rho_{v,e}P_{v,e}}{12\mu_{v,e}l_{eff}}$	*(no)*	$\dot{q}=\frac{r_v L\rho_v P_v}{16\mu_v l_{eff}}$	$q_v=\frac{A_v r_v^2\lambda\rho_v P_v}{16\mu_v L_{eff}}$	[16]
Sonic	$Q_s=0.474 A_v h_{fg}(\rho_v P_v)^{0.5}$	$Q_s=0.474\lambda A_v(\rho_v P_v)^{1/2}$	$\dot{q}=0.474L(\rho_v P_v)^{0.5}$	$q_s=A_v\rho_v\lambda(\frac{\gamma_v R_v T_v}{2(\gamma_v+1)})^{1/2}$	[16]
Capillary	$Q_c=\frac{\sigma_l\rho_l h_{fg}}{\mu_l}\frac{K A_w}{l_{eff}}\left(\frac{2}{r_{c,e}}-\frac{\rho_l g l_t\cos\Psi}{\sigma_l}\right)$	*(no)*	$\dot{Q}_{max}=\left[\frac{\rho_l\sigma_l L}{\mu_l}\right]\left[\frac{KA}{l}\right]\left[\frac{2}{r_c}-\frac{\rho_l g l}{\sigma_l}\sin\phi\right]$	$q\le\frac{\frac{2\sigma}{r_w}-\rho_l g(d_v\cos\psi+L_{eff}\sin\psi)}{(\frac{C f_v\,\mathrm{Re}_v\,\mu_v}{2r_{hv}^2 A_v\rho_v\lambda}+\frac{\mu_l}{K A_w\lambda\rho_l})L_{eff}}$	[15]
Entrainment	$Q_e=A_v h_{fg}\left(\frac{\rho_v\delta_l}{2r_{c,me}}\right)^{0.5}$	$Q_e=A_v\lambda\left(\frac{\sigma\rho_v}{2r_c}\right)^{0.5}$	$\dot{q}=\sqrt{\frac{2\pi\rho_v L^2\sigma_l}{z}}$	$q_e=A_v\lambda(\frac{\sigma\rho_v}{2r_{hv}})^{1/2}$	[16]
Boiling	$Q_b=\frac{4\pi L_{eff}\lambda_{eff}T_v\sigma_v}{h_{fg}\rho_v\ln\frac{r_i}{r_v}}\left(\frac{1}{r_n}-\frac{1}{r_{c,e}}\right)$	$Q_b=\frac{2\pi L_{eff}k_{eff}T_v}{A_v h_{fg}\rho_v\ln(r_i/r_v)}\left[\frac{2\sigma}{r_n}-(\Delta P_c)_{max}\right]$	*(no)*	$q_b=(\frac{2\pi L_e k_{eff}T_v}{\lambda\rho_v\ln(r_i/r_v)})(\frac{2\sigma}{r_n}-\Delta P_{c,in})$	[16]

2.2. Model Validation

Figs. 1(a) and 1(b) show comparisons between the model's prediction and literatures' data. The comparative data in Fig. 1(a) is from [16] for a copper-water heat pipe, with diameter of 20 mm, the total length of 750 mm, the evaporation length of 250 mm, the condensation length of 250 mm, the thickness of tube of 2.5 mm, mesh wicks (100 mesh and 3 layers), and horizontal placement. The data in Fig. 1(b) is from [17] for a water heat pipe, with diameter of 6 mm, the total length of 305 mm, the evaporation length of 25 mm, the condensation length of 76 mm, and horizontal placement.

It is observed that tendencies agree well for all the five limitations in both cases, although there are some differences in quantity. In addition, it is close for the values of the capillary limitations in both cases. This is important because the capillary limitation is generally regarded as the maximum heat transfer capacity, and it is also true as shown in Figs. 1(a) and 1(b) except for at high temperatures. It should be noted that the boiling limitations of the model are about one order of magnitude lower than that in [16] and [17]. Authors conjecture the difference might come from the temperature-dependent property of working fluids, which have not been revealed in [16] and [17]. Overall speaking, in authors' viewpoint, the simple mathematical model is somewhat trustworthy.

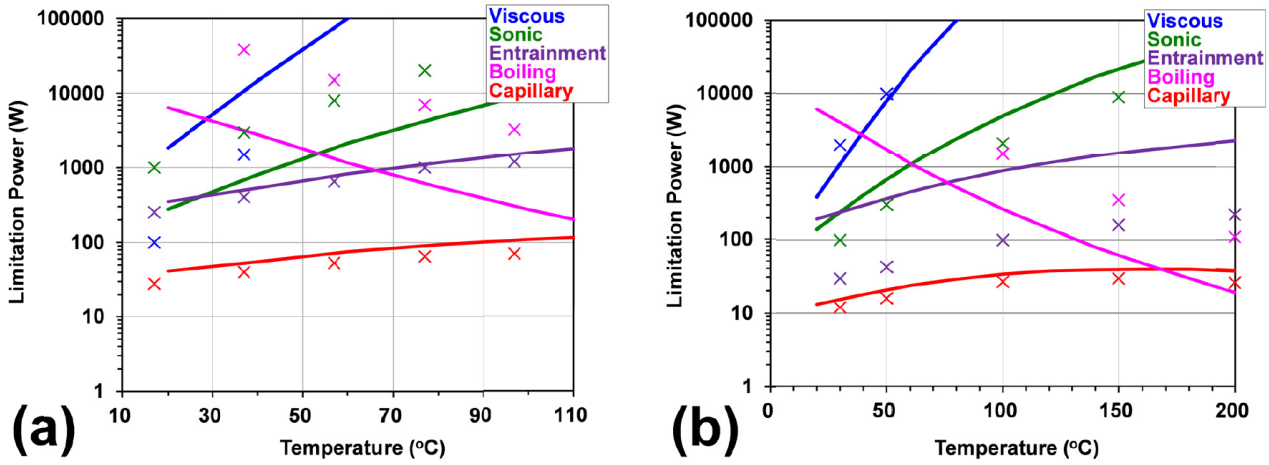

Fig. 1. Model validations, {lines} this study, {points} reference data, (a) data from [16]; (b) data from [17].

3. Case Study

The maximum heat transfer capacity is greatly affected by the size of heat pipes. The size of heat pipes should be varied depending on the purpose of applications. It is impossible to study all of cases in one paper. The paper, hence, pays attention only on the air-to-air heat pipe heat exchanger. The base case of heat pipes is set as follow, heat pipes with water as the working fluid, of outer diameter of 10 mm, the tube thickness of 0.5 mm, the total length of 2000 mm, the evaporation and condensation lengths of both 980 mm, mesh wicks (100 mesh and 1 layer), and vertical placement (hot side in the bottom).

3.1. Influence of the inclination angle and the evaporation temperature on the heat transfer

The influences of the evaporation temperature and the placement angle on the heat transfer capacity are plotted in Figs. 2 and 3. At ψ=0° (horizontal placement) as shown in Fig. 2a, the maximum capacity is mainly governed by the capillary limitation for most of temperatures, except for T>180°C by the boiling limitation. At ψ=45° (Fig. 2b), the maximum capacity is determined by the capillary limitation as T<90°C, and by the boiling limitation as T>90°C. At ψ=90° (Fig. 2c), the maximum capacity is regulated by the entrainment limitation as T<85°C, and by the boiling limitation as T>85°C.

To better understanding of influence of the axial angle on the heat transfer limitations, the data in Fig. 2 are replotted as illustrated in Fig. 3. Three evaporation temperatures of 25, 75, and 150 °C are shown in Figs. 3(a), 3(b), and 3(c), respectively.

Fig. 4 depicts the maximum heat transfer capacity (Q_{max}), which is the lowest quantity of the five limitations. The higher inclination angle, the greater Q_{max} is observed. There exists an optimal Q_{max} for temperatures ranging

from 20 to 200 °C, and the peak of Q_{max} shifts to low temperatures as the increase of inclination angle. These facts reveal complication of heat pipe design.

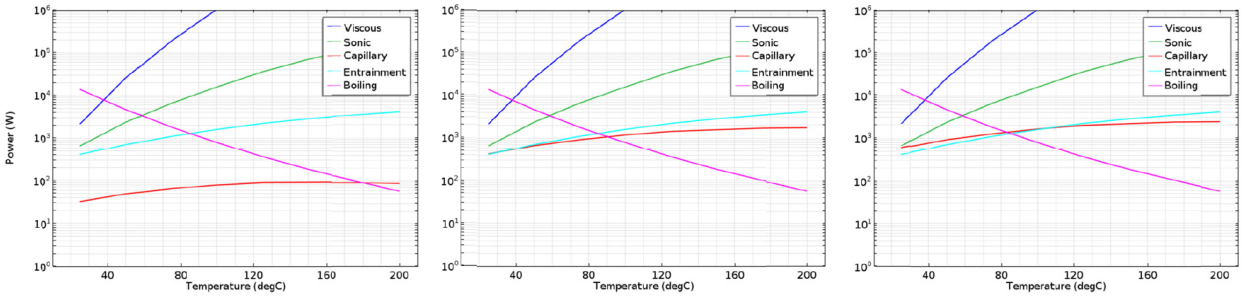

Fig. 2. Relationships between the heat transfer limitations and the temperature for selected axial angles (ψ) of (a) 0°; (b) 45°; (c) 90°.

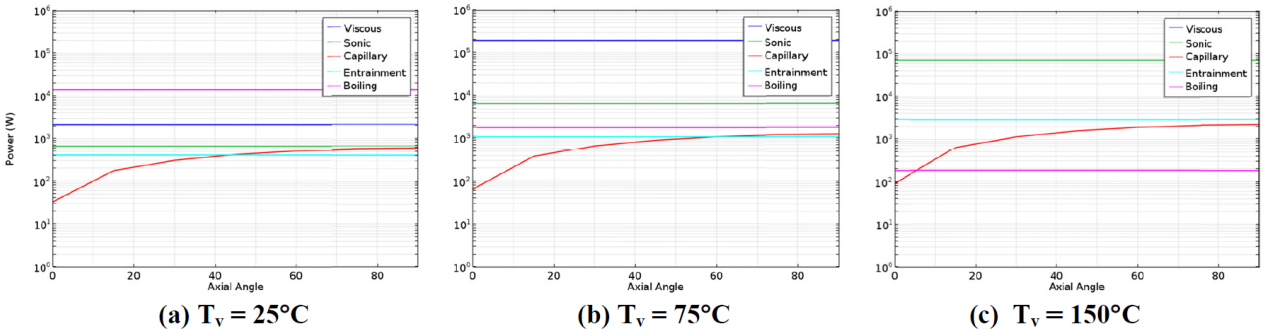

Fig. 3. Relationships between the heat transfer limitations and the axial angle for selected evaporation temperatures of (a) 25°C; (b) 75°C; (c) 150°C.

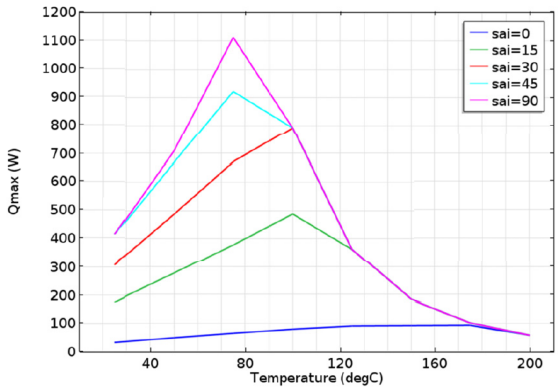

Fig. 4. Relationships between the maximum heat transfer capacity and the evaporation temperature for selected placement angles from 0 to 90°.

3.2. Influence of the mesh wicks on the heat transfer

The influence of the mesh wick on the heat transfer is simulated hereafter. Two factors including the mesh number and the mesh layer are examined. The mesh number ranges from 20 to 500 in^{-1}, and the mesh layer varies from 1 to 5. Results are shown in Figs. 5-7. Nonmonotonic trends between Q_{max} and the mesh number / the mesh

layer are found, and the influences strongly vary with the temperature. In general, but not always true, the lower the mesh layer, the higher Q_{max} is achieved. An optimal mesh number is observed around 100 in^{-1}.

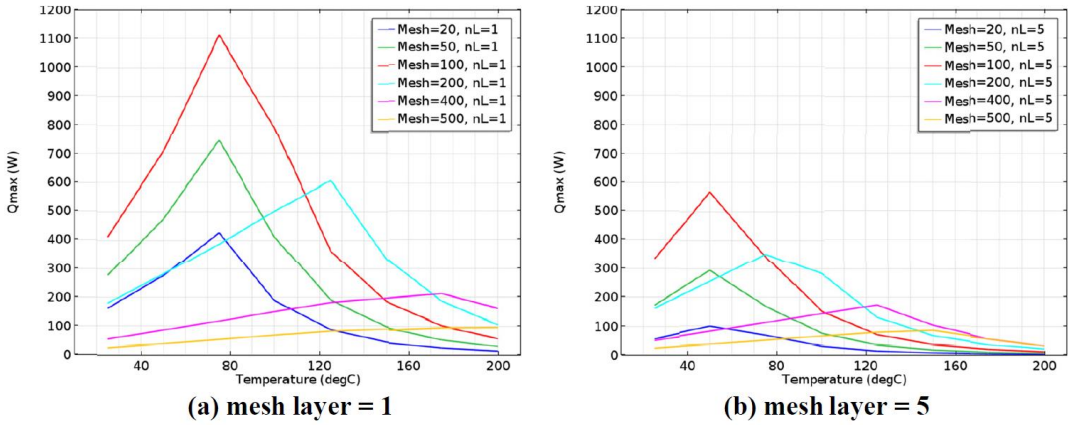

Fig. 5. Influence of the temperature on Q_{max} for selected mesh numbers, (a) the mesh layer, nL=1; (b) the mesh layer, nL=5.

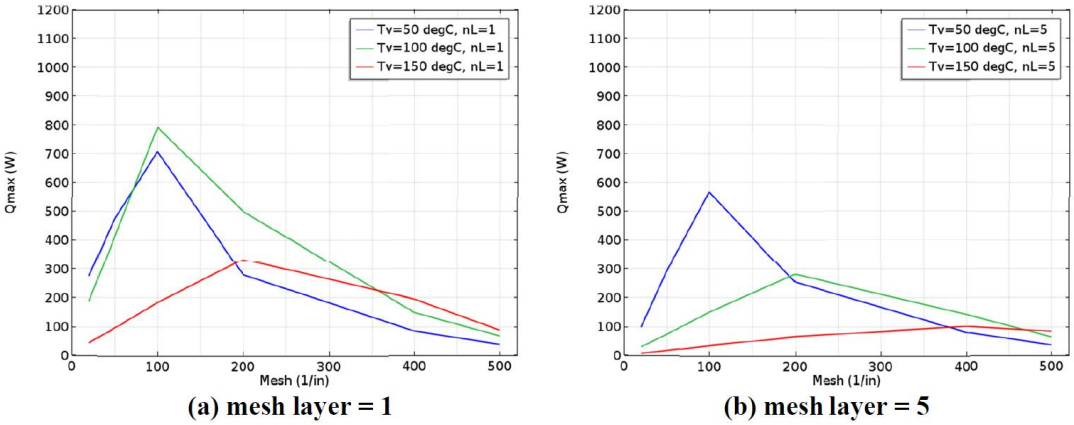

Fig. 6. Influence of the mesh number on Q_{max} for selected temperatures, (a) the mesh layer, nL =1; (b) the mesh layer, nL=5.

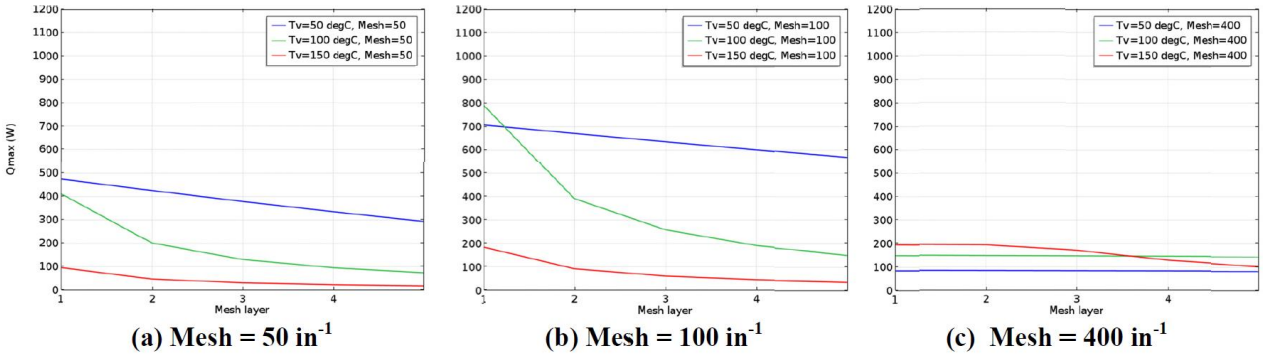

Fig. 7. Influence of the mesh layer on Q_{max} for selected temperatures, (a) mesh=50; (b) mesh=100; (c) mesh=400.

4. Conclusions

A simple mathematical model has been proposed for quick estimation of the maximum heat transfer capacity of tubular water heat pipes with mesh wicks. The prediction agrees well with literature data. A case study of a 2 meter long heat pipe for air-to-air heat exchanger application was performed. The influence of the evaporation temperature, the inclination angle, the mesh number, and the mesh layer on the maximum heat transfer capacity (Q_{max}) was analyzed. Results showed that their trends were nonmonotonic and complicated, and highly depending on the evaporation temperature. The simple mathematical model could serve as a handy tool for quick evaluation of Q_{max} as well as for speedup of a heat pipe design.

Acknowledgements

Funding by the Ministry of Science and Technology (MOST) as well as the Institute of Nuclear Energy Research (INER) are gratefully acknowledged.

References

[1] Energy Procedia-ScienceDirect.com, http://www.sciencedirect.com/science/journal/18766102, (by April 28, 2017).
[2] Kamel, M.S.; Syeal, R.A.; Abdulhussein, A.A.; "Heat transfer enhancement using nanofluids: a review of the recent literature," American Journal of Nano Research and Applications, 4(1), 1–5 (2016).
[3] Mohandas, A.; Dayma, A.S.; "A review on effects of nanofluids on thermal performance of heat pipes," International Journal on Recent and Innovation Trends in Computing and Communication, 4(4), 350–353, (2016).
[4] Sagar, R.; Himanshu, R.; Deepak, A.; Shivade, K.; "A review on effect of nanofluid on the performance heat pipe," International Journal of Advance Research in Science and Engineering, 5(S2) 484–490 (2016).
[5] Shah, B.; "Recent trends in heat pipe applications: a review," International Journal of Science, Engineering and Technology Research (IJSETR), 5(7), 2508–2510 (2016).
[6] Shelke, V.; Yadav, R.J.; Girase, S.B.; "A review of heat pipe systems for heat recovery and renewable energy application," International Journal of Current Engineering and Technology, S4, 102–107 (March 2016).
[7] Smith, M.M.; Aber, J.G.; Rynk, R.; "Heat recovery from composting: a comprehensive review of system design, recovery rate, and utilization," Compost Science & Utilization, DOI: 10.1080/1065657X.2016.1233082 (2016).
[8] Tiwari, M.; Diwakar, N.; "A review of experimental study and CFD based simulation of closed loop pulsating heat pipe," International Journal of Research–Granthaalayah, 4(7), 265–270 (2016).
[9] Vijayakumar, P; Sajairaj, S.; Santhoshkumar, R.; "Review on conventional, modern heat pipes and its applications," International Research Journal of Engineering and Technology (IRJET), 3(10), 513–518 (2016).
[10] Lee, H.M.; Tsai, M.C.; Chen, H.L.; Li, H.Y.; "Stainless steel heat pipe fabrication, performance testing and modeling," Energy Procedia, Vol.105, 2017. *(in press)*
[11] Tsai, M.C.; Wang, H.; Wu, F.H.; Lee, H.M.; Li, H.Y.; Kang, S.W.; "Study of thermal characteristics in a reverse thermosyphon loop," Joint 18th IHPC and 12th IHPS, Jeju, Korea, June 12-16, 2016.
[12] Kang, S.W.; "Preliminary study of solar concentrating high temperature liquid metal heat pipe," Research report of Institute of Nuclear Energy Research (INER-A3134R), Taoyuan City, Taiwan, (2015). *(in Chinese)*
[13] Nemec, P.; Hužvár, J.; "Mathematical calculation of total heat power of sodium heat pipe," Materials Science and Technology, 77-82 (2011).
[14] Bejan, A.; Kraus, A.D.; "Chapter 16, Heat Pipes" in "Heat Transfer Handbook," Wiley, ISBN: 978-0-471-39015-2 (2003).
[15] Reay, D.A.; Kew, P.A.; "Heat Pipes –Theory, Design and Applications," Elsevier, 5th Ed., ISBN: 978-0-7506-6754-8 (2006).
[16] Küçük, S.; "A comparative investigation of heat transfer capacity limits of heat pipes," Master Thesis, Mechanical Engineering Department, Middle East Technical University, Turkey (2007).
[17] PSC Thermal Solutions Co., http://pscmf.com/product/product.php?lang=en&class1=9&class2=21, (available at 2017.03.13).